Triple-charm molecular states composed of D^*D^*D and $D^*D^*D^*$

Si-Qiang Luo,[1,2] Tian-Wei Wu,[3] Ming-Zhu Liu,[4,5] Li-Sheng Geng,[5,6,7,8,*] and Xiang Liu[1,8,9,10,†]

[1]School of Physical Science and Technology, Lanzhou University, Lanzhou 730000, China
[2]School of mathematics and statistics, Lanzhou University, Lanzhou 730000, China
[3]School of Fundamental Physics and Mathematical Sciences, Hangzhou Institute for Advanced Study, UCAS, Hangzhou 310024, China
[4]School of Space and Environment, Beihang University, Beijing 102206, China
[5]School of Physics, Beihang University, Beijing 102206, China
[6]Beijing Key Laboratory of Advanced Nuclear Materials and Physics, Beihang University, Beijing 102206, China
[7]School of Physics and Microelectronics, Zhengzhou University, Zhengzhou, Henan 450001, China
[8]Lanzhou Center for Theoretical Physics, Lanzhou University, Lanzhou 730000, China
[9]Research Center for Hadron and CSR Physics, Lanzhou University and Institute of Modern Physics of CAS, Lanzhou 730000, China
[10]Key Laboratory of Theoretical Physics of Gansu Province, and Frontiers Science Center for Rare Isotopes, Lanzhou University, Lanzhou 730000, China

(Received 3 January 2022; accepted 7 April 2022; published 28 April 2022)

Inspired by the newly observed T_{cc}^+ state, we systematically investigate the S-wave triple-charm molecular states composed of D^*D^*D and $D^*D^*D^*$. We employ the one-boson-exchange model to derive the interactions between $D(D^*)$ and D^* and solve the three-body Schrödinger equations with the Gaussian expansion method. The S-D mixing and coupled channel effects are carefully assessed in our study. Our results show that the $I(J^P) = \frac{1}{2}(0^-, 1^-, 2^-)D^*D^*D$ and $I(J^P) = \frac{1}{2}(0^-, 1^-, 2^-, 3^-)D^*D^*D^*$ systems could form bound states, which can be viewed as three-body hadronic molecules. We present not only the binding energies of the three-body bound states, but also the root-mean-square radii of D-D^* and D^*-D^*, which further corroborate the molecular nature of these states. These predictions could be tested in the future at LHC or HL-LHC.

DOI: 10.1103/PhysRevD.105.074033

I. INTRODUCTION

As important members of the hadron family, exotic states have always interested both theoreticians and experimentalists. By definition, exotic states contain more complex quark and gluon contents than the conventional $q\bar{q}$ mesons and qqq baryons. Given their peculiar nature, studies of exotic states have been a hot topic in hadron physics.

Among the various exotic states, hadronic molecules are quite distinct. They are loosely bound states composed of two or several conventional hadrons and provide a good laboratory to study hadron structure and nonperturbative strong interactions at hadronic level. In 2003, the *BABAR* Collaboration observed a charmed-strange state $D_{s0}^*(2317)$ in the $D_s\pi^0$ channel [1]. Soon after, the CLEO Collaboration not only confirmed its existence, but also found a new charmed-strange state $D_{s1}'(2460)$ in the $D_s^*\pi^0$ mass spectrum [2]. In the same year, the Belle Collaboration reported a hidden-charm state $X(3872)$ in the $J/\psi\pi^+\pi^-$ channel [3]. The $D_{s0}^*(2317)$, $D_{s1}'(2460)$, and $X(3872)$ states have two peculiar features. The first is that their masses are about 100 MeV below the potential model predictions, which implies that it is difficult to categorize them as conventional mesons. The second is that $D_{s0}^*(2317)$, $D_{s1}'(2460)$, and $X(3872)$ are close to and lower than the DK, D^*K, and $D\bar{D}^*$ thresholds, which strongly hints at their molecular nature. Although there are still many controversies, hadronic molecules are one of the most popular interpretations of these exotic hadrons [4–15]. The observations of $D_{s0}^*(2317)$, $D_{s1}'(2460)$, and $X(3872)$ opened a new era in searches for exotic states. In the following years, a plethora of hidden-charm XYZ and P_c states were observed in experiments (for reviews, see Refs. [16–22]).

Very recently, the LHCb Collaboration observed a T_{cc}^+ state in the $D^0D^0\pi^+$ channel [23,24], whose mass and width obtained from a Breit-Wigner fit are

*lisheng.geng@buaa.edu.cn
†xiangliu@lzu.edu.cn

$$m_{\rm BW} = (m_{D^{*+}} + m_{D^0}) - 273 \pm 61 \pm 5^{+11}_{-14}\ \text{keV},$$
$$\Gamma_{\rm BW} = 410 \pm 165 \pm 43^{+18}_{-38}\ \text{keV}. \quad (1)$$

On the other hand, the pole position is given as [24]

$$m_{\rm pole} = (m_{D^{*+}} + m_{D^0}) - 360 \pm 40^{+4}_{-0}\ \text{keV},$$
$$\Gamma_{\rm pole} = 48 \pm 2^{+0}_{-14}\ \text{keV}. \quad (2)$$

From the decay products of T_{cc}^+, one can infer its minimum quark component to be $cc\bar{u}\,\bar{d}$. Since the mass of the T_{cc}^+ is very close to the D^*D threshold, it could well be interpreted as a D^*D molecular state [25–30] as predicted in many previous works [31–34]. As early as in the 1980s, the likely existence of stable tetraquark states has attracted the interests of theorists [35–40]. Latter, various models with different quark-quark interactions were employed to study the mass spectrum of tetraquark states with the $QQ\bar{q}\,\bar{q}$ configuration [41–50]. It should be noted that the T_{cc}^+ is the first observed double-charm exotic state. It is interesting to note that the decay width obtained from the Breit-Wigner fit and that derived from the pole position are quite different. The latter strongly supports its nature being a hadronic molecule of DD^*, as stressed, e.g., in Ref. [51].

The single-charm, hidden-charm, and double-charm molecular candidates have been established in experiments. In Fig. 1, we choose the $D_{s0}^*(2317)$, $X(3872)$, and T_{cc}^+ states as examples and present the corresponding possible substructure. However, until now, there was no signal of triple-charm molecular states. In the future, experimental searches for triple-charm molecular states will be an interesting topic in exploring exotic hadrons.

In this work, we investigate the likely existences of triple-charm molecular states composed of D^*D^*D and $D^*D^*D^*$. There are three reasons for studying such systems. First, we notice that single- and double-charm molecular candidates in Fig. 1 contain one and two charmed mesons, respectively. Thus it is natural to ask whether there exist hadronic molecular states composed of three charmed mesons. Second, the observation of the T_{cc}^+ state provides a way to fix the interaction between two charmed mesons. In Ref. [30], we successfully reproduced the binding energy of the T_{cc}^+ state, with the DD^* interaction provided by the one-boson-exchange (OBE) model. This makes the numerical results more reliable when dealing with systems containing more charmed mesons in the following study. Third, in Ref. [30], we have studied the DDD^* system and found that it has a $I(J^P) = \frac{1}{2}(1^-)$ bound state solution. Compared with the DDD^* system, the D^*D^*D and $D^*D^*D^*$ systems can have more spin configurations. Therefore, it is likely that there exist more hadronic molecular states in the D^*D^*D and $D^*D^*D^*$ systems.

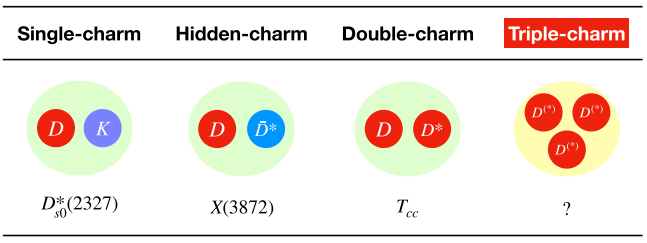

FIG. 1. Various types of hadronic molecular candidates. Here, we choose $D_{s0}^*(2317)$, $X(3872)$, and T_{cc} as examples.

In the past several years, the LHCb Collaboration has achieved great success in discovering exotic states, including several P_c states [52,53], P_{cs} [54], $X_{0,1}(2900)$ [55,56], and $X(6900)$ [57]. These observations demonstrated the capacity of the LHCb detector in searching for exotic states. With the upgrade of the LHCb detector [58], one can expect that more exotic states will be observed in the future. The predictions of molecular states with the configurations of D^*D^*D and $D^*D^*D^*$ may inspire more experimental works along this line.

This paper is organized as follows. In Sec. II, we introduce the interactions between D^* and $D^{(*)}$ and present the details of the Gaussian expansion method. Next in Sec. III, we present the binding energies and root-mean-square radii of the D^*D^*D and $D^*D^*D^*$ systems. Finally, this paper ends with a short summary in Sec. IV.

II. FORMALISM

In order to study the D^*D^*D and $D^*D^*D^*$ systems, we should first derive the effective potentials of the D^*-D^* and D-D^* pairs. For this purpose, we adopt the OBE model of Ref. [33]. In the OBE model, the D^*-$D^{(*)}$ interactions occur by the scattering process as shown in Fig. 2, where we should consider the exchanges of π, σ, ρ, and ω mesons. Then, in the momentum space, the effective potential related to the scatting amplitude can be written as

$$V^{h_1h_2\to h_3h_4}(\mathbf{q}) = -\frac{\mathcal{M}^{h_1h_2\to h_3h_4}(\mathbf{q})}{\sqrt{\prod_i 2m_i \prod_i 2m_f}}, \quad (3)$$

where $\mathcal{M}^{h_1h_2\to h_3h_4}(\mathbf{q})$ is the scattering amplitude. The m_i and m_f are masses of the initial and final states. To take into the finite size of the exchanged mesons, a monopole form factor is introduced

$$\mathcal{F}(q^2, m_E^2) = \frac{\Lambda^2 - m_E^2}{\Lambda^2 - q^2}, \quad (4)$$

where q and m_E are the mass and momentum of the exchanged meson, respectively. The effective potentials in the coordinate space can be obtained by the following Fourier transformation:

$$V^{h_1h_2\to h_3h_4}(\mathbf{r}) = \int \frac{\mathrm{d}^3\mathbf{q}}{(2\pi)^3} e^{i\mathbf{q}\cdot\mathbf{r}} V^{h_1h_2\to h_3h_4}(\mathbf{q}) \mathcal{F}^2(q^2, m_E^2). \quad (5)$$

In the following, we present the effective potentials of the $D^* - D^{(*)}$ interactions explicitly, i.e.,

$$
\begin{aligned}
V^{DD^*\to DD^*} &= -g_\sigma^2\mathcal{O}_1 Y_\sigma + \frac{1}{2}\beta^2 g_V^2\mathcal{O}_1(\mathcal{C}_1(I)Y_\rho + \mathcal{C}_0(I)Y_\omega),\\
V^{DD^*\to D^*D} &= \frac{g^2}{3f_\pi^2}(\mathcal{O}_2\hat{\mathcal{P}} + \mathcal{O}_3\hat{\mathcal{Q}})\mathcal{C}_1'(I)Y_{\pi 1} + \frac{2}{3}\lambda^2 g_V^2(2\mathcal{O}_2\hat{\mathcal{P}} - \mathcal{O}_3\hat{\mathcal{Q}})(\mathcal{C}_1'(I)Y_{\rho 1} + \mathcal{C}_0'(I)Y_{\omega 1}),\\
V^{DD^*\to D^*D^*} &= \frac{g^2}{3f_\pi^2}(\mathcal{O}_4\hat{\mathcal{P}} + \mathcal{O}_5\hat{\mathcal{Q}})\mathcal{C}_1(I)Y_{\pi 2} + \frac{2}{3}\lambda^2 g_V^2(2\mathcal{O}_4\hat{\mathcal{P}} - \mathcal{O}_5\hat{\mathcal{Q}})(\mathcal{C}_1(I)Y_{\rho 2} + \mathcal{C}_0(I)Y_{\omega 2}),\\
V^{D^*D^*\to D^*D^*} &= -g_\sigma^2\mathcal{O}_6 Y_\sigma + \frac{1}{2}\beta^2 g_V^2\mathcal{O}_6(\mathcal{C}_1(I)Y_\rho + \mathcal{C}_0(I)Y_\omega) - \frac{g^2}{3f_\pi^2}(\mathcal{O}_7\hat{\mathcal{P}} + \mathcal{O}_8\hat{\mathcal{Q}})\mathcal{C}_1(I)Y_\pi\\
&\quad - \frac{2}{3}\lambda^2 g_V^2(2\mathcal{O}_7\hat{\mathcal{P}} - \mathcal{O}_8\hat{\mathcal{Q}})(\mathcal{C}_1(I)Y_\rho + \mathcal{C}_0(I)Y_\omega).
\end{aligned}
\tag{6}
$$

In Eq. (6), the $\mathcal{O}_i$'s are spin-dependent operators, which are defined as

$$
\begin{aligned}
\mathcal{O}_1 &= \boldsymbol{\epsilon}_4^\dagger\cdot\boldsymbol{\epsilon}_2,\\
\mathcal{O}_2 &= \boldsymbol{\epsilon}_3^\dagger\cdot\boldsymbol{\epsilon}_2,\\
\mathcal{O}_3 &= S(\mathbf{r},\boldsymbol{\epsilon}_3^\dagger,\boldsymbol{\epsilon}_2),\\
\mathcal{O}_4 &= \boldsymbol{\epsilon}_3^\dagger\cdot(i\boldsymbol{\epsilon}_4^\dagger\times\boldsymbol{\epsilon}_2),\\
\mathcal{O}_5 &= S(\mathbf{r},\boldsymbol{\epsilon}_3^\dagger, i\boldsymbol{\epsilon}_4^\dagger\times\boldsymbol{\epsilon}_2),\\
\mathcal{O}_6 &= (\boldsymbol{\epsilon}_3^\dagger\cdot\boldsymbol{\epsilon}_1)(\boldsymbol{\epsilon}_4^\dagger\cdot\boldsymbol{\epsilon}_2),\\
\mathcal{O}_7 &= (\boldsymbol{\epsilon}_3^\dagger\times\boldsymbol{\epsilon}_1)\cdot(\boldsymbol{\epsilon}_4^\dagger\times\boldsymbol{\epsilon}_2),\\
\mathcal{O}_8 &= S(\mathbf{r},\boldsymbol{\epsilon}_3^\dagger\times\boldsymbol{\epsilon}_1,\boldsymbol{\epsilon}_4^\dagger\times\boldsymbol{\epsilon}_2),
\end{aligned}
\tag{7}
$$

where

$$
S(\mathbf{r},\mathbf{a},\mathbf{b}) = \frac{3(\mathbf{a}\cdot\mathbf{r})(\mathbf{b}\cdot\mathbf{r})}{r^2} - \mathbf{a}\cdot\mathbf{b} \tag{8}
$$

is the tensor operator. Here, $\boldsymbol{\epsilon}_i$ $(i = 1, 2)$ and $\boldsymbol{\epsilon}_i^\dagger$ $(i = 3, 4)$ are initial and final polarization vectors of the D^* mesons, respectively, and $C_0^{(\prime)}(I)$ and $C_1^{(\prime)}(I)$ are flavor-dependent factors given by

$$
\begin{aligned}
&\mathcal{C}_1(0) = -\frac{3}{2}, \quad \mathcal{C}_1'(0) = +\frac{3}{2}, \quad \mathcal{C}_0(0) = +\frac{1}{2}, \quad \mathcal{C}_0'(0) = -\frac{1}{2},\\
&\mathcal{C}_1(1) = +\frac{1}{2}, \quad \mathcal{C}_1'(1) = +\frac{1}{2}, \quad \mathcal{C}_0(1) = +\frac{1}{2}, \quad \mathcal{C}_0'(1) = +\frac{1}{2}.
\end{aligned}
\tag{9}
$$

The function Y_i in Eq. (6) is written as[1]

[1]In momentum space, the effective potentials share a common part, i.e.,

$$
V(\mathbf{q}) = \frac{1}{\mathbf{q}^2 + m_E^2 - q^{02}}, \tag{10}
$$

where the q^0 is energy component of the exchanged momentum, whose explicit expression could be found in Ref. [32]. Without a form factor, the Fourier transformation of Eq. (10) is

$$
V(\mathbf{r}) = \int\frac{\mathrm{d}^3\mathbf{q}}{(2\pi)^3}\mathrm{e}^{i\mathbf{q}\cdot\mathbf{r}}\frac{1}{\mathbf{q}^2 + m_E^2 - q^{02}} = \frac{1}{4\pi r}\mathrm{e}^{-\sqrt{m_E^2 - q^{02}}r}. \tag{11}
$$

After introducing the form factor, the Fourier transformation is

$$
V(\mathbf{r}) = \int\frac{\mathrm{d}^3\mathbf{q}}{(2\pi)^3}\mathrm{e}^{i\mathbf{q}\cdot\mathbf{r}}\frac{1}{\mathbf{q}^2 + m_E^2 - q^{02}}\mathcal{F}^2(q^2, m_E^2). \tag{12}
$$

After performing the integration, one could obtain the function Y_i given in Eq. (13).

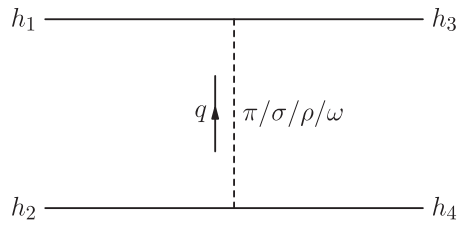

FIG. 2. The Feynman diagrams for the $h_1h_2 \to h_3h_4$ process. In this work, the h_1, h_2, h_3, and h_4 are $D^{(*)}$ mesons.

$$Y_i = \frac{e^{-m_{Ei}r}}{4\pi r} - \frac{e^{-\Lambda_i r}}{4\pi r} - \frac{\Lambda_i^2 e^{-\Lambda_i r}}{8\pi\Lambda_i} + \frac{m_{Ei}^2 e^{-\Lambda_i r}}{8\pi\Lambda_i} \tag{13}$$

with $\Lambda_i = \sqrt{\Lambda^2 - q_i^2}$ and $m_{Ei} = \sqrt{m_E^2 - q_i^2}$. The q_i is the energy component of the exchanged momentum. We employ $q_1 = m_{D^*} - m_D$ and $q_2 = (m_{D^*}^2 - m_D^2)/(4m_{D^*})$ for the $DD^* \to D^*D$ and $DD^* \to D^*D^*$ processes, respectively. The operators $\hat{\mathcal{P}}$ and $\hat{\mathcal{Q}}$ only act on Y_i and the expressions are

$$\hat{\mathcal{P}} = \frac{1}{r^2}\frac{\partial}{\partial r}r^2\frac{\partial}{\partial r}, \qquad \hat{\mathcal{Q}} = r\frac{\partial}{\partial r}\frac{1}{r}\frac{\partial}{\partial r}. \tag{14}$$

To evaluate the above potentials, we also need the values of the coupling constants and the masses of the mesons, which are collected in Table I.

To solve the three-body Schrödinger equation, we employ the Gaussian expansion method [63,64], which was widely used in studies of baryon systems [65–67], multiquark states [68–72], and multibody hadronic molecular states [30,73–76] (for reviews on this latter topic, see, e.g., Refs. [77,78]). The three-body Schrödinger equation reads

$$[\hat{T} + V(r_1) + V(r_2) + V(r_3)]\Psi_{JM} = E\Psi_{JM}, \tag{15}$$

where $\hat{T}$ is the kinetic energy operator, and $V(r_1)$, $V(r_2)$, and $V(r_3)$ are pairwise potentials. Ψ_{JM} is the total wave function, which can be written as

$$\Psi_{JM} = \sum_{c,\alpha} C_{c,\alpha}\Psi_{JM}^{(c,\alpha)}, \tag{16}$$

TABLE I. Values of the coupling constants [33,59–61] and meson masses [62].

Coupling Constants	Values	Mesons	Mass (GeV)
g	0.6	π	0.140
f_π	0.132 GeV	σ	0.600
g_σ	3.4	ρ	0.770
βg_V	5.2	ω	0.780
λg_V	3.133 GeV^{-1}	D	1.867
		D^*	2.009

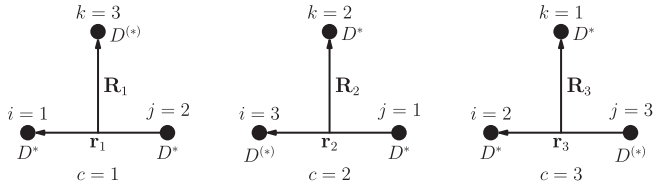

FIG. 3. Jacobi coordinates of the $D^*D^*D^{(*)}$ systems.

where

$$\Psi_{JM}^{(c,\alpha)} = H_{t,T}^c[\chi_{s,S}^c[\phi_{nl}(\mathbf{r}_c)\phi_{NL}(\mathbf{R}_c)]_\lambda]_{JM} \tag{17}$$

is the basis, and $C_{c,\alpha}$ is the coefficient of the corresponding basis, which can be obtained by the Rayleigh-Ritz variational method. The c ($c = 1, 2, 3$) represents the three channels in Fig. 3 and $\alpha = \{tT, sS, nN, lL\lambda\}$ is the quantum number of the basis. $H_{t,T}^c$ is the flavor wave function, where t is isospin in the $\mathbf{r}_c$ degree of freedom and T is the total isospin. $\chi_{s,S}^c$ is the spin wave function, where the s, S are spin in the $\mathbf{r}_c$ degree of freedom and total spin, respectively. $\phi_{nlm_l}(\mathbf{r}_c)$ and $\phi_{NLM_L}(\mathbf{R}_c)$ are spatial wave functions, which read

$$\begin{aligned}\phi_{nlm_l}(\mathbf{r}_c) &= N_{nl}r_c^l e^{-\nu_n r_c^2}Y_{lm}(\hat{\mathbf{r}}_c),\\ \phi_{NLM_L}(\mathbf{R}_c) &= N_{NL}R_c^L e^{-\lambda_N R_c^2}Y_{LM}(\hat{\mathbf{R}}_c),\end{aligned} \tag{18}$$

where N_{nl} and N_{NL} are normalization constants. In Eq. (18), The $\mathbf{r}_c$ and $\mathbf{R}_c$ are Jacobi coordinates, and ν_n and λ_N are Gaussian ranges. After the above preparations, we can calculate the kinetic, potential, and normalization matrix elements (see Refs. [63,79] for more details), i.e.,

$$\begin{aligned}T_{\alpha\alpha'}^{ab} &= \langle\Psi_{JM}^{(a,\alpha)}|\hat{T}|\Psi_{JM}^{(b,\alpha')}\rangle,\\ V_{\alpha\alpha' c}^{ab} &= \langle\Psi_{JM}^{(a,\alpha)}|V(r_c)|\Psi_{JM}^{(b,\alpha')}\rangle,\\ N_{\alpha\alpha'}^{ab} &= \langle\Psi_{JM}^{(a,\alpha)}|\Psi_{JM}^{(b,\alpha')}\rangle.\end{aligned} \tag{19}$$

Then, Eq. (15) could be further expressed as the following general eigenvalue equation:

$$\left(T_{\alpha\alpha'}^{ab} + \sum_{c=1}^{3} V_{\alpha\alpha' c}^{ab}\right)C_{b,\alpha'} = EN_{\alpha\alpha'}^{ab}C_{b,\alpha'}. \tag{20}$$

III. NUMERICAL RESULTS

With the effective potentials of Eq. (6), we could solve the three-body Schrödinger equation with the Gaussian expansion method. We not only calculate the binding energies, but also obtain the root-mean-square radii of D^*-D^* and D-D^*. In general, orbitally excited hadronic molecular states are more difficult to be formed because of

the repulsive centrifugal potential of the discussed systems. It is more likely to find bound state solutions from the S-wave ($l = L = 0$) configurations in most situations. In the first step, we only consider the S-wave contributions. Then the S-D mixing effect is included in the realistic calculation. When the S-D mixing effect is introduced, the tensor terms from the π, ρ, and ω contribute to the potential matrix elements. In the nuclear system, the tensor terms play an important role in the nucleon-nucleon interactions [80–83]. Similar results could be found in the charmed baryon-charmed baryon system [84], where the tensor force from the S-D mixing is necessary for obtaining the bound state solutions. Thus, in this work, we also consider the tensor terms. Besides the S-D mixing and tensor terms, the coupled channel effect cannot be ignored when calculating the binding energy of a bound state [32,85]. Since both the D^*D^*D and $D^*D^*D^*$ systems can have the quantum numbers $I(J^P) = \frac{1}{2}(0^-, 1^-, 2^-)$ and $I(J^P) = \frac{3}{2}(0^-, 1^-, 2^-)$, we should consider the D^*D^*D-$D^*D^*D^*$ coupled channel effect, which plays a role in the $DD^* \to D^*D^*$ or the $D^*D^* \to DD^*$ process.

In our approach, the cutoff Λ is a crucial parameter when searching for the bound state solutions of these discussed systems. With the measured binding energy of the T_{cc}^+ state, we obtained $\Lambda = 0.976$, 0.998, and 1.013 GeV in Ref. [30], which are close to the suggested values in previous works [32,86–90]. The D^*D^*D and $D^*D^*D^*$ systems can be related to the DDD^* system via heavy quark spin symmetry. As a result, in this work we will take the same strategy as that of Ref. [30]; i.e., we scan the range of Λ from 0.90 to 3.0 GeV to search for bound states of D^*D^*D and $D^*D^*D^*$. If a system has a bound state solution with $\Lambda \approx 1$ GeV, we view this state as a good molecular candidate.

In the study of hadronic molecular candidates composed of two charmed mesons [32], it was found that systems with lower isospins are more likely to bind. In this work, we find that this is also true for systems composed of three charmed mesons.

A. D^*D^*D system

For the S-wave only D^*D^*D system, allowed spin parities are 0^-, 1^-, and 2^- with $I = \frac{1}{2}$ and $\frac{3}{2}$. In the S-D mixing scheme, we require $l + L \leq 2$ to restrict the maximum orbital angular momentum. It should be noted that for the D^*-D^* pair, the sum of $t + s + l$ should be odd. In Table II, we present the configurations of the D^*D^*D-$D^*D^*D^*$ system. For the S-wave only and the S-D mixing schemes of the D^*D^*D system, we calculate the binding energies and root-mean-square radii for $I(J^P) = \frac{1}{2}(0^-, 1^-, 2^-)$ and $I(J^P) = \frac{3}{2}(0^-, 1^-, 2^-)$. In the coupled-channel case of D^*D^*D-$D^*D^*D^*$, we present the binding energies and probabilities of the D^*D^*D and $D^*D^*D^*$. The numerical results are shown in Table III.

For the S-wave only D^*D^*D system with $I(J^P) = \frac{1}{2}(0^-)$, we can obtain bound state solutions when the cutoff Λ reaches about 0.98 GeV. The binding energy is on the order of MeV and the root-mean-square radii are several fm. If we increase the cutoff Λ, the binding energy increases while the root-mean-square radii decrease. We note that the consideration of S-D mixing and the coupled-channel ($D^*D^*D^*$) effect increases the binding energy, which is reflected by the fact that a slightly smaller cutoff is needed to obtain a binding energy similar to the case for which only the S-wave interaction is taken into account. For the cutoff range studied, the probability of the $D^*D^*D^*$ configuration is small and at the order of a few percent. Since the binding energy and root-mean-square radii are reasonable from the perspective of hadronic molecules, this state could be viewed as a good hadronic molecular candidate.

For the S-wave only D^*D^*D system with $I(J^P) = \frac{1}{2}(1^-)$, we can also obtain bound state solutions with the cutoff $\Lambda = 0.98$, 1.03, and 1.08 GeV. Further consideration of the S-D mixing and $D^*D^*D^*$ coupled-channel effect does not change the overall picture. According to the calculated binding energy and root-mean-square radii, this state could also be treated as an ideal hadronic molecular candidate.

For the S-wave only D^*D^*D system with $I(J^P) = \frac{1}{2}(2^-)$, one can also find weakly bound states for the same cutoff Λ as that of $I(J^P) = \frac{1}{2}(0^-, 1^-)$. Similar to the case of $P_c(4440)$ and $P_c(4457)$, for the same cutoff, the 0^-, 1^-, 2^- states have different binding energies at the order of several hundred keV. With increased experimental precision, it is likely that these states can be distinguished from each other in future experiments. The contribution of the S-D mixing and coupled-channel effect is also similar to the case of $I(J^P) = \frac{1}{2}(0^-, 1^-)$.

We also study the D^*D^*D system for $I(J^P) = \frac{3}{2}(0^-, 1^-, 2^-)$. There are no bound state solutions for a cutoff Λ below 1.013 GeV. In order to obtain bound state solutions for the S-wave only D^*D^*D systems with $I(J^P) = \frac{3}{2}(0^-, 1^-2^-)$, we increase the cutoff Λ to 1.76–1.86 GeV, 1.85–1.95 GeV, and 1.49–1.59 GeV, respectively. Here, we increase the cutoff in steps of 0.05 GeV when scanning the cutoff Λ. Similar results are also obtained when the S-D mixing and coupled channel effect are taken into account. Considering that the needed cutoff Λ is out of the range of 0.976–1.013 GeV (the range determined in Ref. [30]), we are a bit reluctant to view the $I(J^P) = \frac{3}{2}(0^-, 1^-, 2^-)D^*D^*D$ bound states as good hadronic molecular candidates.

We note an interesting scenario in the S-D mixing scheme for the $I(J^P) = \frac{3}{2}(1^-)$ case. When the cutoff Λ changes from 1.85 GeV to 1.90 GeV, $r_{D^*D^*}$ decreases from 11.98 fm to 1.88 fm, while r_{D^*D} increases from 8.80 fm to 14.38 fm. For the S-D mixing $I(J^P) = \frac{3}{2}(1^-)D^*D^*D$ state, there are more than one bound states. For convenience, we

TABLE II. Configurations of the $D^*D^*D - D^*D^*D^*$ systems. The $R^c_{lL\lambda} = [\phi_{nl}(\mathbf{r}_c)\phi_{NL}(\mathbf{R}_c)]_\lambda$, χ^c_{sS}, and H^c_{fT} represent the spatial, spin, and flavor wave functions, respectively.

		D^*D^*D		$D^*D^*D^*$
I	J^P	$c = 1$	$c = 2,\ 3$	$c = 1,\ 2,\ 3$
$\frac{1}{2}$	0^-	$R^c_{202}\chi^c_{2,2}H^c_{1,\frac{1}{2}}, R^c_{022}\chi^c_{2,2}H^c_{1,\frac{1}{2}}, R^c_{112}\chi^c_{2,2}H^c_{0,\frac{1}{2}}, R^c_{000}\chi^c_{0,0}H^c_{1,\frac{1}{2}}, R^c_{111}\chi^c_{1,1}H^c_{1,\frac{1}{2}}, R^c_{110}\chi^c_{0,0}H^c_{0,\frac{1}{2}}$	$R^c_{202}\{\chi^c_{1,2}H^c_{0,\frac{1}{2}}, \chi^c_{1,2}H^c_{1,\frac{1}{2}}\}, R^c_{022}\{\chi^c_{1,2}H^c_{0,\frac{1}{2}}, \chi^c_{1,2}H^c_{1,\frac{1}{2}}\}, R^c_{112}\{\chi^c_{1,2}H^c_{0,\frac{1}{2}}, \chi^c_{1,2}H^c_{1,\frac{1}{2}}\}, R^c_{000}\{\chi^c_{1,0}H^c_{0,\frac{1}{2}}, \chi^c_{1,0}H^c_{1,\frac{1}{2}}\}, R^c_{111}\{\chi^c_{1,1}H^c_{0,\frac{1}{2}}, \chi^c_{1,1}H^c_{1,\frac{1}{2}}\}, R^c_{110}\{\chi^c_{1,0}H^c_{0,\frac{1}{2}}, \chi^c_{1,0}H^c_{1,\frac{1}{2}}\}$	$R^c_{000}\chi^c_{1,0}H^c_{0,\frac{1}{2}}, R^c_{110}\chi^c_{1,0}H^c_{1,\frac{1}{2}}, R^c_{202}\{\chi^c_{1,2}H^c_{0,\frac{1}{2}}, \chi^c_{2,2}H^c_{1,\frac{1}{2}}\}, R^c_{022}\{\chi^c_{1,2}H^c_{0,\frac{1}{2}}, \chi^c_{2,2}H^c_{1,\frac{1}{2}}\}, R^c_{112}\{\chi^c_{1,2}H^c_{1,\frac{1}{2}}, \chi^c_{2,2}H^c_{0,\frac{1}{2}}\}, R^c_{111}\{\chi^c_{0,1}H^c_{0,\frac{1}{2}}, \chi^c_{1,1}H^c_{1,\frac{1}{2}}, \chi^c_{2,1}H^c_{0,\frac{1}{2}}\}$
	1^-	$R^c_{000}\chi^c_{1,1}H^c_{0,\frac{1}{2}}, R^c_{110}\chi^c_{1,1}H^c_{1,\frac{1}{2}}, R^c_{202}\{\chi^c_{1,1}H^c_{0,\frac{1}{2}}, \chi^c_{2,2}H^c_{1,\frac{1}{2}}\}, R^c_{022}\{\chi^c_{1,1}H^c_{0,\frac{1}{2}}, \chi^c_{2,2}H^c_{1,\frac{1}{2}}\}, R^c_{112}\{\chi^c_{1,1}H^c_{1,\frac{1}{2}}, \chi^c_{2,2}H^c_{0,\frac{1}{2}}\}, R^c_{111}\{\chi^c_{0,0}H^c_{0,\frac{1}{2}}, \chi^c_{1,1}H^c_{1,\frac{1}{2}}, \chi^c_{2,2}H^c_{0,\frac{1}{2}}\}$	$R^c_{000}\{\chi^c_{1,1}H^c_{0,\frac{1}{2}}, \chi^c_{1,1}H^c_{1,\frac{1}{2}}\}, R^c_{110}\{\chi^c_{1,1}H^c_{0,\frac{1}{2}}, \chi^c_{1,1}H^c_{1,\frac{1}{2}}\}, R^c_{202}\{\chi^c_{1,1}H^c_{0,\frac{1}{2}}, \chi^c_{1,2}H^c_{0,\frac{1}{2}}, \chi^c_{1,1}H^c_{1,\frac{1}{2}}, \chi^c_{1,2}H^c_{1,\frac{1}{2}}\}, R^c_{022}\{\chi^c_{1,1}H^c_{0,\frac{1}{2}}, \chi^c_{1,2}H^c_{0,\frac{1}{2}}, \chi^c_{1,1}H^c_{1,\frac{1}{2}}, \chi^c_{1,2}H^c_{1,\frac{1}{2}}\}, R^c_{112}\{\chi^c_{1,1}H^c_{0,\frac{1}{2}}, \chi^c_{1,2}H^c_{0,\frac{1}{2}}, \chi^c_{1,1}H^c_{1,\frac{1}{2}}, \chi^c_{1,2}H^c_{1,\frac{1}{2}}\}, R^c_{111}\{\chi^c_{1,0}H^c_{0,\frac{1}{2}}, \chi^c_{1,1}H^c_{0,\frac{1}{2}}, \chi^c_{1,2}H^c_{0,\frac{1}{2}}, \chi^c_{1,0}H^c_{1,\frac{1}{2}}, \chi^c_{1,1}H^c_{1,\frac{1}{2}}, \chi^c_{1,2}H^c_{1,\frac{1}{2}}\}$	$R^c_{000}\{\chi^c_{0,1}H^c_{1,\frac{1}{2}}, \chi^c_{1,1}H^c_{0,\frac{1}{2}}, \chi^c_{2,1}H^c_{1,\frac{1}{2}}\}, R^c_{110}\{\chi^c_{0,1}H^c_{0,\frac{1}{2}}, \chi^c_{1,1}H^c_{1,\frac{1}{2}}, \chi^c_{2,1}H^c_{0,\frac{1}{2}}\}, R^c_{202}\{\chi^c_{0,1}H^c_{1,\frac{1}{2}}, \chi^c_{1,1}H^c_{0,\frac{1}{2}}, \chi^c_{1,2}H^c_{0,\frac{1}{2}}, \chi^c_{2,1}H^c_{1,\frac{1}{2}}, \chi^c_{2,2}H^c_{1,\frac{1}{2}}, \chi^c_{2,3}H^c_{1,\frac{1}{2}}\}, R^c_{022}\{\chi^c_{0,1}H^c_{1,\frac{1}{2}}, \chi^c_{1,1}H^c_{0,\frac{1}{2}}, \chi^c_{1,2}H^c_{0,\frac{1}{2}}, \chi^c_{2,1}H^c_{1,\frac{1}{2}}, \chi^c_{2,2}H^c_{1,\frac{1}{2}}, \chi^c_{2,3}H^c_{1,\frac{1}{2}}\}, R^c_{112}\{\chi^c_{0,1}H^c_{0,\frac{1}{2}}, \chi^c_{1,1}H^c_{1,\frac{1}{2}}, \chi^c_{1,2}H^c_{1,\frac{1}{2}}, \chi^c_{2,1}H^c_{0,\frac{1}{2}}, \chi^c_{2,2}H^c_{0,\frac{1}{2}}, \chi^c_{2,3}H^c_{0,\frac{1}{2}}\}, R^c_{111}\{\chi^c_{0,1}H^c_{0,\frac{1}{2}}, \chi^c_{1,0}H^c_{1,\frac{1}{2}}, \chi^c_{1,1}H^c_{1,\frac{1}{2}}, \chi^c_{1,2}H^c_{1,\frac{1}{2}}, \chi^c_{2,1}H^c_{0,\frac{1}{2}}, \chi^c_{2,2}H^c_{0,\frac{1}{2}}\}$
	2^-	$R^c_{000}\chi^c_{2,2}H^c_{1,\frac{1}{2}}, R^c_{110}\chi^c_{2,2}H^c_{0,\frac{1}{2}}, R^c_{111}\{\chi^c_{1,1}H^c_{1,\frac{1}{2}}, \chi^c_{2,2}H^c_{0,\frac{1}{2}}\}, R^c_{202}\{\chi^c_{0,0}H^c_{1,\frac{1}{2}}, \chi^c_{1,1}H^c_{0,\frac{1}{2}}, \chi^c_{2,2}H^c_{1,\frac{1}{2}}\}, R^c_{022}\{\chi^c_{0,0}H^c_{1,\frac{1}{2}}, \chi^c_{1,1}H^c_{0,\frac{1}{2}}, \chi^c_{2,2}H^c_{1,\frac{1}{2}}\}, R^c_{112}\{\chi^c_{0,0}H^c_{0,\frac{1}{2}}, \chi^c_{1,1}H^c_{1,\frac{1}{2}}, \chi^c_{2,2}H^c_{0,\frac{1}{2}}\}$	$R^c_{000}\{\chi^c_{1,2}H^c_{0,\frac{1}{2}}, \chi^c_{1,2}H^c_{1,\frac{1}{2}}\}, R^c_{110}\{\chi^c_{1,2}H^c_{0,\frac{1}{2}}, \chi^c_{1,2}H^c_{1,\frac{1}{2}}\}, R^c_{111}\{\chi^c_{1,1}H^c_{0,\frac{1}{2}}, \chi^c_{1,2}H^c_{0,\frac{1}{2}}, \chi^c_{1,1}H^c_{1,\frac{1}{2}}, \chi^c_{1,2}H^c_{1,\frac{1}{2}}\}, R^c_{202}\{\chi^c_{1,0}H^c_{0,\frac{1}{2}}, \chi^c_{1,1}H^c_{0,\frac{1}{2}}, \chi^c_{1,2}H^c_{0,\frac{1}{2}}, \chi^c_{1,0}H^c_{1,\frac{1}{2}}, \chi^c_{1,1}H^c_{1,\frac{1}{2}}, \chi^c_{1,2}H^c_{1,\frac{1}{2}}\}, R^c_{022}\{\chi^c_{1,0}H^c_{0,\frac{1}{2}}, \chi^c_{1,1}H^c_{0,\frac{1}{2}}, \chi^c_{1,2}H^c_{0,\frac{1}{2}}, \chi^c_{1,0}H^c_{1,\frac{1}{2}}, \chi^c_{1,1}H^c_{1,\frac{1}{2}}, \chi^c_{1,2}H^c_{1,\frac{1}{2}}\}, R^c_{112}\{\chi^c_{1,0}H^c_{0,\frac{1}{2}}, \chi^c_{1,1}H^c_{0,\frac{1}{2}}, \chi^c_{1,2}H^c_{0,\frac{1}{2}}, \chi^c_{1,0}H^c_{1,\frac{1}{2}}, \chi^c_{1,1}H^c_{1,\frac{1}{2}}, \chi^c_{1,2}H^c_{1,\frac{1}{2}}\}$	$R^c_{000}\{\chi^c_{1,2}H^c_{0,\frac{1}{2}}, \chi^c_{2,2}H^c_{1,\frac{1}{2}}\}, R^c_{110}\{\chi^c_{1,2}H^c_{1,\frac{1}{2}}, \chi^c_{2,2}H^c_{0,\frac{1}{2}}\}, R^c_{111}\{\chi^c_{0,1}H^c_{0,\frac{1}{2}}, \chi^c_{1,1}H^c_{1,\frac{1}{2}}, \chi^c_{1,2}H^c_{1,\frac{1}{2}}, \chi^c_{2,1}H^c_{0,\frac{1}{2}}, \chi^c_{2,2}H^c_{0,\frac{1}{2}}, \chi^c_{2,3}H^c_{0,\frac{1}{2}}\}, R^c_{202}\{\chi^c_{0,1}H^c_{1,\frac{1}{2}}, \chi^c_{1,0}H^c_{0,\frac{1}{2}}, \chi^c_{1,1}H^c_{0,\frac{1}{2}}, \chi^c_{1,2}H^c_{0,\frac{1}{2}}, \chi^c_{2,1}H^c_{1,\frac{1}{2}}, \chi^c_{2,2}H^c_{1,\frac{1}{2}}, \chi^c_{2,3}H^c_{1,\frac{1}{2}}\}, R^c_{022}\{\chi^c_{0,1}H^c_{1,\frac{1}{2}}, \chi^c_{1,0}H^c_{0,\frac{1}{2}}, \chi^c_{1,1}H^c_{0,\frac{1}{2}}, \chi^c_{1,2}H^c_{0,\frac{1}{2}}, \chi^c_{2,1}H^c_{1,\frac{1}{2}}, \chi^c_{2,2}H^c_{1,\frac{1}{2}}, \chi^c_{2,3}H^c_{1,\frac{1}{2}}\}, R^c_{112}\{\chi^c_{0,1}H^c_{0,\frac{1}{2}}, \chi^c_{1,0}H^c_{1,\frac{1}{2}}, \chi^c_{1,1}H^c_{1,\frac{1}{2}}, \chi^c_{1,2}H^c_{1,\frac{1}{2}}, \chi^c_{2,1}H^c_{0,\frac{1}{2}}, \chi^c_{2,2}H^c_{0,\frac{1}{2}}, \chi^c_{2,3}H^c_{0,\frac{1}{2}}\}$
	3^-			$R^c_{000}\chi^c_{2,3}H^c_{1,\frac{1}{2}}, R^c_{110}\chi^c_{2,3}H^c_{0,\frac{1}{2}}, R^c_{111}\{\chi^c_{1,2}H^c_{1,\frac{1}{2}}, \chi^c_{2,2}H^c_{0,\frac{1}{2}}, \chi^c_{2,3}H^c_{0,\frac{1}{2}}\}, R^c_{202}\{\chi^c_{0,1}H^c_{1,\frac{1}{2}}, \chi^c_{1,1}H^c_{0,\frac{1}{2}}, \chi^c_{1,2}H^c_{0,\frac{1}{2}}, \chi^c_{2,1}H^c_{1,\frac{1}{2}}, \chi^c_{2,2}H^c_{1,\frac{1}{2}}, \chi^c_{2,3}H^c_{1,\frac{1}{2}}\}, R^c_{022}\{\chi^c_{0,1}H^c_{1,\frac{1}{2}}, \chi^c_{1,1}H^c_{0,\frac{1}{2}}, \chi^c_{1,2}H^c_{0,\frac{1}{2}}, \chi^c_{2,1}H^c_{1,\frac{1}{2}}, \chi^c_{2,2}H^c_{1,\frac{1}{2}}, \chi^c_{2,3}H^c_{1,\frac{1}{2}}\}, R^c_{112}\{\chi^c_{0,1}H^c_{0,\frac{1}{2}}, \chi^c_{1,1}H^c_{1,\frac{1}{2}}, \chi^c_{1,2}H^c_{1,\frac{1}{2}}, \chi^c_{2,1}H^c_{0,\frac{1}{2}}, \chi^c_{2,2}H^c_{0,\frac{1}{2}}, \chi^c_{2,3}H^c_{0,\frac{1}{2}}\}$
$\frac{3}{2}$	0^-	$R^c_{202}\chi^c_{2,2}H^c_{1,\frac{3}{2}}, R^c_{000}\chi^c_{0,0}H^c_{1,\frac{3}{2}}, R^c_{022}\chi^c_{2,2}H^c_{1,\frac{3}{2}}, R^c_{111}\chi^c_{1,1}H^c_{1,\frac{3}{2}}$	$R^c_{202}\chi^c_{1,2}H^c_{1,\frac{3}{2}}, R^c_{022}\chi^c_{1,2}H^c_{1,\frac{3}{2}}, R^c_{112}\chi^c_{1,2}H^c_{1,\frac{3}{2}}, R^c_{000}\chi^c_{1,0}H^c_{1,\frac{3}{2}}, R^c_{111}\chi^c_{1,1}H^c_{1,\frac{3}{2}}, R^c_{110}\chi^c_{1,0}H^c_{1,\frac{3}{2}}$	$R^c_{202}\chi^c_{2,2}H^c_{1,\frac{3}{2}}, R^c_{022}\chi^c_{2,2}H^c_{1,\frac{3}{2}}, R^c_{112}\chi^c_{1,2}H^c_{1,\frac{3}{2}}, R^c_{111}\chi^c_{1,1}H^c_{1,\frac{3}{2}}, R^c_{110}\chi^c_{1,0}H^c_{1,\frac{3}{2}}$
	1^-	$R^c_{202}\chi^c_{2,2}H^c_{1,\frac{3}{2}}, R^c_{022}\chi^c_{2,2}H^c_{1,\frac{3}{2}}, R^c_{112}\chi^c_{1,1}H^c_{1,\frac{3}{2}}, R^c_{111}\chi^c_{1,1}H^c_{1,\frac{3}{2}}, R^c_{110}\chi^c_{1,1}H^c_{1,\frac{3}{2}}$	$R^c_{000}\chi^c_{1,1}H^c_{1,\frac{3}{2}}, R^c_{110}\chi^c_{1,1}H^c_{1,\frac{3}{2}}, R^c_{202}\{\chi^c_{1,1}H^c_{1,\frac{3}{2}}, \chi^c_{1,2}H^c_{1,\frac{3}{2}}\}, R^c_{022}\{\chi^c_{1,1}H^c_{1,\frac{3}{2}}, \chi^c_{1,2}H^c_{1,\frac{3}{2}}\}, R^c_{112}\{\chi^c_{1,1}H^c_{1,\frac{3}{2}}, \chi^c_{1,2}H^c_{1,\frac{3}{2}}\}, R^c_{111}\{\chi^c_{1,0}H^c_{1,\frac{3}{2}}, \chi^c_{1,1}H^c_{1,\frac{3}{2}}, \chi^c_{1,2}H^c_{1,\frac{3}{2}}\}$	$R^c_{000}\{\chi^c_{0,1}H^c_{1,\frac{3}{2}}, \chi^c_{2,1}H^c_{1,\frac{3}{2}}\}, R^c_{110}\chi^c_{1,1}H^c_{1,\frac{3}{2}}, R^c_{112}\{\chi^c_{1,1}H^c_{1,\frac{3}{2}}, \chi^c_{1,2}H^c_{1,\frac{3}{2}}\}, R^c_{111}\{\chi^c_{1,0}H^c_{1,\frac{3}{2}}, \chi^c_{1,1}H^c_{1,\frac{3}{2}}, \chi^c_{1,2}H^c_{1,\frac{3}{2}}\}, R^c_{202}\{\chi^c_{0,1}H^c_{1,\frac{3}{2}}, \chi^c_{2,1}H^c_{1,\frac{3}{2}}, \chi^c_{2,2}H^c_{1,\frac{3}{2}}, \chi^c_{2,3}H^c_{1,\frac{3}{2}}\}, R^c_{022}\{\chi^c_{0,1}H^c_{1,\frac{3}{2}}, \chi^c_{2,1}H^c_{1,\frac{3}{2}}, \chi^c_{2,2}H^c_{1,\frac{3}{2}}, \chi^c_{2,3}H^c_{1,\frac{3}{2}}\}$
	2^-	$R^c_{000}\chi^c_{2,2}H^c_{1,\frac{3}{2}}, R^c_{112}\chi^c_{1,1}H^c_{1,\frac{3}{2}}, R^c_{111}\chi^c_{1,1}H^c_{1,\frac{3}{2}}, R^c_{202}\{\chi^c_{0,0}H^c_{1,\frac{3}{2}}, \chi^c_{2,2}H^c_{1,\frac{3}{2}}\}, R^c_{022}\{\chi^c_{0,0}H^c_{1,\frac{3}{2}}, \chi^c_{2,2}H^c_{1,\frac{3}{2}}\}$	$R^c_{000}\chi^c_{1,2}H^c_{1,\frac{3}{2}}, R^c_{110}\chi^c_{1,2}H^c_{1,\frac{3}{2}}, R^c_{111}\{\chi^c_{1,1}H^c_{1,\frac{3}{2}}, \chi^c_{1,2}H^c_{1,\frac{3}{2}}\}, R^c_{202}\{\chi^c_{1,0}H^c_{1,\frac{3}{2}}, \chi^c_{1,1}H^c_{1,\frac{3}{2}}, \chi^c_{1,2}H^c_{1,\frac{3}{2}}\}, R^c_{022}\{\chi^c_{1,0}H^c_{1,\frac{3}{2}}, \chi^c_{1,1}H^c_{1,\frac{3}{2}}, \chi^c_{1,2}H^c_{1,\frac{3}{2}}\}, R^c_{112}\{\chi^c_{1,0}H^c_{1,\frac{3}{2}}, \chi^c_{1,1}H^c_{1,\frac{3}{2}}, \chi^c_{1,2}H^c_{1,\frac{3}{2}}\}$	$R^c_{000}\chi^c_{2,2}H^c_{1,\frac{3}{2}}, R^c_{110}\chi^c_{1,2}H^c_{1,\frac{3}{2}}, R^c_{111}\{\chi^c_{1,1}H^c_{1,\frac{3}{2}}, \chi^c_{1,2}H^c_{1,\frac{3}{2}}\}, R^c_{112}\{\chi^c_{1,0}H^c_{1,\frac{3}{2}}, \chi^c_{1,1}H^c_{1,\frac{3}{2}}, \chi^c_{1,2}H^c_{1,\frac{3}{2}}\}, R^c_{202}\{\chi^c_{0,1}H^c_{1,\frac{3}{2}}, \chi^c_{2,1}H^c_{1,\frac{3}{2}}, \chi^c_{2,2}H^c_{1,\frac{3}{2}}, \chi^c_{2,3}H^c_{1,\frac{3}{2}}\}, R^c_{022}\{\chi^c_{0,1}H^c_{1,\frac{3}{2}}, \chi^c_{2,1}H^c_{1,\frac{3}{2}}, \chi^c_{2,2}H^c_{1,\frac{3}{2}}, \chi^c_{2,3}H^c_{1,\frac{3}{2}}\}$
	3^-			$R^c_{000}\chi^c_{2,3}H^c_{1,\frac{3}{2}}, R^c_{111}\chi^c_{1,2}H^c_{1,\frac{3}{2}}, R^c_{112}\{\chi^c_{1,1}H^c_{1,\frac{3}{2}}, \chi^c_{1,2}H^c_{1,\frac{3}{2}}\}, R^c_{202}\{\chi^c_{0,1}H^c_{1,\frac{3}{2}}, \chi^c_{2,1}H^c_{1,\frac{3}{2}}, \chi^c_{2,2}H^c_{1,\frac{3}{2}}, \chi^c_{2,3}H^c_{1,\frac{3}{2}}\}, R^c_{022}\{\chi^c_{0,1}H^c_{1,\frac{3}{2}}, \chi^c_{2,1}H^c_{1,\frac{3}{2}}, \chi^c_{2,2}H^c_{1,\frac{3}{2}}, \chi^c_{2,3}H^c_{1,\frac{3}{2}}\}$

TABLE III. Binding energies, root-mean-square radii, and probabilities of the D^*D^*D system.

		S-wave				*S*-*D* mixing				coupled channels			
I	J^P	Λ (GeV)	B (MeV)	$r_{D^*D^*}$ (fm)	r_{D^*D} (fm)	Λ (GeV)	B (MeV)	$r_{D^*D^*}$ (fm)	r_{D^*D} (fm)	Λ (GeV)	B (MeV)	$P_{D^*D^*D}$ (%)	$P_{D^*D^*D^*}$ (%)
$\frac{1}{2}$	0^-	0.98	0.45	7.73	6.11	0.95	0.44	7.64	6.08	0.92	0.84	99.34	0.66
		1.03	3.60	3.91	3.03	1.00	3.38	3.81	2.98	0.97	5.44	97.95	2.05
		1.08	9.65	2.55	1.99	1.05	9.10	2.51	1.97	1.02	14.79	95.86	4.14
	1^-	0.98	0.86	3.52	3.88	0.95	0.44	5.11	5.25	0.93	0.81	99.29	0.71
		1.03	6.84	1.55	1.82	1.00	5.16	1.81	2.11	0.98	6.22	97.95	2.05
		1.08	17.43	1.10	1.31	1.05	14.21	1.23	1.46	1.03	18.03	95.50	4.50
	2^-	0.97	0.82	4.36	3.67	0.94	0.57	5.34	4.45	0.90	0.48	99.26	0.74
		1.02	6.30	2.00	1.71	0.99	5.04	2.28	1.94	0.95	7.05	96.32	3.68
		1.07	16.19	1.41	1.22	1.04	13.54	1.56	1.35	1.00	22.16	91.42	8.58
$\frac{3}{2}$	0^-	1.76	0.41	5.26	4.44	1.75	0.37	5.33	4.52	1.76	0.63	99.99	0.01
		1.81	1.94	3.27	2.70	1.80	1.81	3.31	2.74	1.81	2.28	99.98	0.02
		1.86	4.48	2.50	2.03	1.85	4.21	2.52	2.06	1.86	4.91	99.98	0.02
	1^-	1.85	0.46	11.75	8.68	1.85	0.54	11.98	8.80	1.85	0.57	∼100	∼0
		1.90	2.20	11.23	8.09	1.90	2.41	1.88	14.38	1.90	2.41	∼100	∼0
		1.95	4.97	10.93	7.81	1.95	5.61	1.35	14.26	1.95	5.61	∼100	∼0
	2^-	1.49	0.86	2.26	2.29	1.48	0.66	2.48	2.51	1.47	0.31	99.97	0.03
		1.54	5.16	1.32	1.34	1.53	4.48	1.39	1.42	1.52	3.68	99.96	0.04
		1.59	12.46	0.98	1.00	1.58	11.10	1.03	1.04	1.57	9.70	99.96	0.04

use s_1 to denote the bound state solution with $r_{D^*D^*} \approx 11$ fm and $r_{D^*D} \approx 8$ fm, and s_2 to label the bound state solution with $r_{D^*D^*} \approx 2$ fm and $r_{D^*D} \approx 14$ fm. The dependence of the two solutions s_1 and s_2 on the cutoff Λ is found to be different. However, in Table III, we only show the bound state solutions with the largest binding energy. With $\Lambda = 1.85$ GeV, we found that $B_{s1} > B_{s2}$; thus, we show the bound state solution s_1. While for $\Lambda = 1.90$ and 1.95 GeV, we present the bound state solution s_2 since $B_{s1} < B_{s2}$.

If only the *S*-wave interaction had been considered for the $I(J^P) = \frac{3}{2}(1^-)D^*D^*D$ state, only the bound state solution s_1 would have been obtained. Thus, the *S*-*D* mixing effect plays a significant role for this state. Further studies of the *S*-*D* mixing effect shows that the bound state solution s_2 is highly correlated to the configuration $R^1_{022}\chi^1_{2,2}H^1_{1,\frac{3}{2}}$ (see Table II). This could be diagnosed in the following steps:

(1) In the *S*-*D* mixing scheme without the $R^1_{022}\chi^1_{2,2}H^1_{1,\frac{3}{2}}$ configuration, the bound state solution s_1 exists but not the s_2 solution.
(2) In the *S*-wave only combing with the $R^1_{022}\chi^1_{2,2}H^1_{1,\frac{3}{2}}$ configuration, both solutions s_1 and s_2 exist.
(3) If only the configuration $R^1_{022}\chi^1_{2,2}H^1_{1,\frac{3}{2}}$ is considered, only the solution s_2 exists.

From the above analysis, we conclude that the $R^1_{022}\chi^1_{2,2}H^1_{1,\frac{3}{2}}$ configuration affects the results and contributes dominantly to the bound state solution s_2.

How to search for D^*D^*D molecular candidates is also an interesting question. One possible decay mode is that the triple-charm molecules decay into a double-charm molecular state and a charmed meson. The other possible mode is that they directly decay into multibody final states bypassing intermediate states. Here, we summarize these channels as follows.

(i) If the binding energies are extremely small, they could first decay into $T^+_{cc}D^*$, and then T^+_{cc} can decay into $DD\pi$, and D^* could be seen in the $D\pi$ and $D\gamma$ channels. In this case, the molecular candidates may be observed in the $DDD\pi\pi$ and $DDD\pi\gamma$ final states.
(ii) If the masses of the molecular candidates are below the $T^+_{cc}D^*$ threshold, the kinematically allowed channel is $T^+_{cc}D$. The D^*D^*D molecular candidates could be studied in the $DDD\pi$ channel.
(iii) If the D^*D^* hadronic molecular state exists, the D^*D^*D molecular candidates may decay into a D^*D^* molecular state and D. The D^*D^* molecular state could be observed in the D^*D, $DD\pi$, and $DD\gamma$ final states.
(iv) In the above three scenarios, the D^*D^*D molecular candidates ultimately decay into three charmed mesons together with π and γ. We should also emphasize that these final states can originate not only from the intermediate double-charm molecular states with $D^{(*)}$, but also from nonresonant processes.
(v) In addition, the D^*D^*D molecular candidates can also decay into three charmed mesons via fall apart or quark rearrangement mechanisms. The typical channels are D^*DD and DDD.

TABLE IV. Binding energies and root-mean-square radii of $D^*D^*D^*$ system.

		S-wave			*S*-*D* Mixing		
I	J^P	Λ (GeV)	B (MeV)	$r_{D^*D^*}$ (fm)	Λ (GeV)	B (MeV)	$r_{D^*D^*}$ (fm)
$\frac{1}{2}$	0^-	1.02	0.67	9.75	1.00	0.84	9.92
		1.07	4.48	9.06	1.05	4.57	9.17
		1.12	10.72	8.81	1.10	10.63	8.88
	1^-	1.00	0.67	5.52	0.97	0.44	6.02
		1.05	5.02	2.51	1.02	4.30	2.61
		1.10	12.83	1.73	1.07	11.52	1.78
	2^-	0.98	0.37	4.71	0.96	0.51	4.53
		1.03	5.94	1.79	1.01	5.80	1.87
		1.08	16.33	1.25	1.06	15.55	1.31
	3^-	1.84	0.51	9.74	1.02	0.35	12.19
		1.89	2.39	9.18	1.07	4.03	11.72
		1.94	5.38	8.90	1.12	10.23	11.63
$\frac{3}{2}$	1^-	1.80	0.20	7.82	1.81	0.46	7.21
		1.85	1.40	6.11	1.86	1.89	5.59
		1.90	3.59	4.92	1.91	4.37	4.45
	2^-	1.85	0.81	9.60	1.84	0.61	9.89
		1.90	2.89	9.13	1.89	2.51	9.29
		1.95	6.13	8.88	1.94	5.53	8.98
	3^-	1.48	0.23	2.95	1.48	0.78	2.31
		1.53	4.21	1.38	1.53	4.90	1.34
		1.58	11.28	1.00	1.58	11.93	1.00

According to the discussions above, the D^*D^*D molecular candidates could be studied with the three-, four-, and five-body final states in future experiments.

B. $D^*D^*D^*$ system

Since the $D^*D^*D^*$ system contains three identical mesons, the $c = 1, 2, 3$ channels share the same configurations. In addition, for all the channels, $(-1)^{t+s+l+1} = 1$, which restricts allowed combinations of t, s, and l. For the S-wave only $D^*D^*D^*$ system with $I = \frac{1}{2}$, the allowed spin parities are 0^-, 1^-, 2^-, and 3^-. For $I = \frac{3}{2}$ in S-wave, the allowed spin parities are 1^-, 2^-, and 3^-. For all the $D^*D^*D^*$ states, we also consider the S-D mixing effect. As shown in Table III, the coupled-channel effects between D^*D^*D-$D^*D^*D^*$ are small and thus could be neglected. We notice that the threshold of $D^*D^*D^*$ is about 140 MeV higher than that of D^*D^*D, and therefore the D^*D^*D component is difficult to be bounded in the $D^*D^*D^*$-predominate states. In general, the coupled-channel effects of D^*D^*D-$D^*D^*D^*$ mainly affect the decay behaviors of the $D^*D^*D^*$ states. Since we focus primarily on the existences of the bound states of $D^*D^*D^*$, the coupled-channel effects of D^*D^*D-$D^*D^*D^*$ are not considered here. The binding energies and root-mean-square radii are presented in Table IV.

For the S-wave only $D^*D^*D^*$ system with $I(J^P) = \frac{1}{2}(0^-)$, we find a bound state solution for a cutoff Λ larger than 1.02 GeV. The root-mean-square radii decrease slowly with the increase of the cutoff Λ. The radius $r_{D^*D^*}$ is estimated to be about 9 fm with $\Lambda \sim 1$ GeV, which is a bit larger than that of T_{cc}^+ but similar to those of the DDD^* states. Judging from the binding energy and root-mean-square radii, this state could be viewed as a good hadronic molecular candidate.

For the S-wave only $D^*D^*D^*$ system with $I(J^P) = \frac{1}{2}(1^-)$, we obtain a binding energy in the range of 0.67–12.83 MeV for a cutoff Λ between 1.00 and 1.10 GeV. While the root-mean-square radii decrease from 5.52 to 1.73 fm with the increase of the cutoff Λ.

For the S-wave only $D^*D^*D^*$ system with $I(J^P) = \frac{1}{2}(2^-)$, the system becomes bound when the cutoff Λ reaches about 0.98 GeV. Since the obtained binding energy is on the order of MeV and the root-mean-square radii are several fm, this state is also an ideal hadronic molecular candidate.

For the three configurations studied, turning on the S-D mixing only has a small effect but, in general, slightly increases the binding energy of the system of interest (for the same cutoff).

For the S-wave only $D^*D^*D^*$ system with $I(J^P) = \frac{1}{2}(3^-)$, there is no bound state solution with a $\Lambda \approx 1$ GeV. But if the S-D mixing is taken into account, we can obtain loosely bound state solutions for a cutoff $\Lambda \approx 1$ GeV. By carefully studying the configurations in the S-D mixing scheme for the case of $I(J^P) = \frac{1}{2}(3^-)D^*D^*D^*$, we find that the configurations of $R^c_{022}\chi^c_{1,1}H^c_{0,\frac{1}{2}}$ and $R^c_{022}\chi^c_{1,2}H^c_{0,\frac{1}{2}}$ ($c = 1$, 2, 3) play a key role in forming bound states. Similar to the analysis performed in studying the $I(J^P) = \frac{3}{2}(2^-)D^*D^*D$ state, the above conclusion is obtained in the following way

(1) In the S-D mixing scheme without $R^c_{022}\chi^c_{1,1}H^c_{0,\frac{1}{2}}$ and $R^c_{022}\chi^c_{1,2}H^c_{0,\frac{1}{2}}$ ($c = 1$, 2, 3), there are no bound state solutions with $\Lambda \approx 1$ GeV.

(2) In the S-wave only combing with $R^c_{022}\chi^c_{1,1}H^c_{0,\frac{1}{2}}$ and $R^c_{022}\chi^c_{1,2}H^c_{0,\frac{1}{2}}$ ($c = 1$, 2, 3), it is easy to find bound state solutions with $\Lambda \approx 1$ GeV and the binding energies are approximate to those in the S-D mixing scheme given in Table IV.

(3) If the $R^c_{022}\chi^c_{1,1}H^c_{0,\frac{1}{2}}$ or $R^c_{022}\chi^c_{1,2}H^c_{0,\frac{1}{2}}$ ($c = 1$, 2, 3) configuration is considered, nearly the same binding energy is obtained as that of the S-D mixing scheme in Table IV when $\Lambda \approx 1$ GeV.

Because of the complexity of the three-body problem, it is difficult to present a precise interpretation for this phenomenon, but some qualitative analyses are helpful to understand the numerical results. For the configurations $R^c_{022}\chi^c_{1,1}H^c_{0,\frac{1}{2}}$ and $R^c_{022}\chi^c_{1,2}H^c_{0,\frac{1}{2}}$ ($c = 1$, 2, 3), the isospin and spin in the $\mathbf{r}_c$ degree of freedom are $t = 0$ and $s = 1$, respectively, and the flavor and spin factors of the π

exchange are $\mathcal{C}_1(0) = -3/2$ and $\langle \mathcal{O}_7 \rangle = 1$ [33], respectively. In this spin-isospin configuration, the D^*-D^* force from the π exchange is attractive and about 3 times of that in the S-wave only scheme with $t = 1$ and $s = 2$. We notice that $R^1_{022}\chi^1_{2,2}H^1_{1,\frac{3}{2}}$ in the D^*D^*D system and $R^c_{022}\chi^c_{1,1}H^c_{0,\frac{1}{2}}$ and $R^c_{022}\chi^c_{1,2}H^c_{0,\frac{1}{2}}$ ($c = 1, 2, 3$) in the $D^*D^*D^*$ system are $\mathbf{R}_c$-mode excited configurations, i.e., $l = 0$, $L = 2$ ($l = 2$, $L = 0$ for the $\mathbf{r}_c$-mode D-wave excited configuration.) Since the reduced mass of the $\mathbf{R}_c$ degree of freedom is larger than that of the $\mathbf{r}_c$ degree of freedom, if we take the same Gaussian variational parameters as inputs, the $\mathbf{R}_c$-mode excited configuration has a smaller kinetic matrix element than that of the $\mathbf{r}_c$-mode excited configuration, which is beneficial to form a $\mathbf{R}_c$-mode excited state. This might be the reason why some $\mathbf{R}_c$-mode excited configurations in the D^*D^*D and $D^*D^*D^*$ systems play a significant role in the S-D mixing scheme.

The three-body system contains two spatial degrees of freedom. If we introduce S-D mixing, a large number of configurations are included in the calculation. For some specific spin-isospin configurations, the π exchange force is attractive. If such spin-flavor configurations emerge in the S-D mixing scheme but not in the S-wave only scenario, we should carefully investigate the S-D mixing effect.

According to the above analysis, it is possible to find D-wave bound state solutions. But in the present work, we mainly focus on molecular states in the S-wave only or S-D mixing scenarios.

For the S-wave only $I(J^P) = \frac{3}{2}(1^-, 2^-, 3^-)D^*D^*D^*$ systems, a larger cutoff is needed for them to bind. More specifically, we only find bound state solutions when the cutoff Λ reaches around 1.8 GeV for $I(J^P) = \frac{3}{2}(1^-, 2^-)$. We also obtain shallow bound states in the S-wave only $I(J^P) = \frac{3}{2}(3^-)D^*D^*D^*$ system if the cutoff Λ is close to 1.5 GeV. Since the needed cutoff Λ is much larger than our expectation, we prefer not to view these states as good hadronic molecular candidates. For all the $I = 3/2$ configurations, the S-D mixing effect is relatively small and plays a minor role.

Since the $D^*D^*D^*$ molecular candidates have larger masses than that of the D^*D^*D system, much more complex decay modes can be anticipated. Here, the decay channels are summarized as the following:

(i) In principle, all the decay modes of the D^*D^*D molecular candidates are also kinematically allowed for the $D^*D^*D^*$ system.

(ii) There are also some modes specific for the $D^*D^*D^*$ system. For example, the channel of a D^*D^* molecular candidate with a D^* meson is only kinematically allowed for the $D^*D^*D^*$ system.

However, although there are more decay channels for the $D^*D^*D^*$ system, the decay patterns are similar for the DDD^* [30], D^*D^*D, and $D^*D^*D^*$ molecular states. In the future, these states could be searched for by measuring three charmed mesons together with pions and photons in the final states.

C. Sensitivity of binding energies to the coupling constants

In addition to the cutoff Λ, the coupling constants which determine the strength of the potentials are also important to determine whether the three mesons can form bound states. In Eq. (6), there are five coupling constants, i.e., g, g_σ, g_V, β, and λ. Among them, only the coupling constant g is determined by the experimental partial decay width $D^* \to D\pi$. All the others are taken from models. For example, g_σ is estimated by the quark model [59], and β is obtained from the vector meson dominance mechanism [61]. Since there exist uncertainties for the involved coupling constants, it is relevant to study the sensitivity of our results to the adopted values of the coupling constants. We notice that the ρ and ω exchange potentials share a common coupling constant g_V. In order to study the sensitivity of the bound state solutions to the coupling constants, we introduce an about 10% uncertainty to them, which is somehow arbitrary but nevertheless reasonable.

The numerical results for the D^*D^*D and $D^*D^*D^*$ systems are presented in Tables V and VI, respectively. We note that the binding energies are highly dependent on the square of the coupling constants, which is easy to understand since all the potentials in Eq. (6) are proportional to the square of the coupling constants. Meanwhile, since the changes of the coupling constants could be viewed as perturbations to the potentials, we estimate the binding energies in perturbation theory. Here, we employ the S-wave only D^*D^*D system with $I(J^P) = \frac{1}{2}(0^-)$ as an example to illustrate this point. As shown in Table V, we obtain a binding energy $B = 3.60$ MeV with a cutoff $\Lambda = 1.03$ GeV. The expectation value of the potential from the π exchange is -16.81 MeV. If we allow g to vary by 10% (0.9–1.1), the square of the ratio is in the range 0.81–1.21. Then the expectation value of the π exchange potential is estimated to be in the range of $-13.63 - -20.34$ MeV. The resulting binding energy is then 0.41–7.13 MeV, which is consistent with the exact result 1.08–7.92 MeV. Following the same approach, when g_σ, βg_V, and λg_V are varied by 10%, the estimated binding energies in leading order perturbation theory are in the ranges of 0.57–6.95 MeV, 2.84–4.44 MeV, 3.29–3.94 MeV, respectively, which are all consistent with the exact values 1.27–7.87 MeV, 2.87–4.47 MeV, 3.30–3.95 MeV, respectively.

The message from the above sensitivity study is that although the exact binding energies are sensitive to the values of the coupling constants, the overall picture remains unchanged, i.e., whether there exist some good three-body hadronic molecules.

TABLE V. Dependence of binding energies on the variation of the coupling constants by about 10% in the D^*D^*D system. The cutoff Λ, potential expectations $\langle V\rangle$, and binding energies $B^{(\prime)}$ are in units of GeV, MeV, and MeV, respectively. The binding energies B are calculated with the values of the coupling constants given in the fifth column, and the B' are obtained within their uncertainties.

					S-wave					*S-D* Mixing					Coupled Channel				
I	J^P	Exchanged Mesons	Coupling constant	Reference value	Λ	B	$\langle V\rangle$	Reference range	B'	Λ	B	$\langle V\rangle$	Reference range	B'	Λ	B	$\langle V\rangle$	Reference range	B'
$\frac{1}{2}$	0^-	π	g	0.6	1.03	3.60	−16.81	0.54–0.66	1.08–7.92	1.00	3.38	−19.16	0.54–0.66	0.68–8.51	0.97	5.44	−32.83	0.54–0.66	0.99–14.58
		σ	g_σ	3.4			−15.96	3.06–3.74	1.27–7.87			−13.73	3.06–3.74	1.34–6.99			−14.95	3.06–3.74	3.02–9.10
		ρ, ω	βg_V	5.2			−3.98	4.68–5.72	2.87–4.47			−2.93	4.68–5.72	2.84–4.02			−3.15	4.68–5.72	4.86–6.12
		ρ, ω	λg_V (GeV^{-1})	3.133			−1.63	2.82–3.45	3.30–3.95			−0.84	2.82–3.45	3.22–3.56			−2.00	2.82–3.45	5.08–5.88
		Kinetic energy $\langle T\rangle$ (MeV)					34.78	...	...			33.28	...	...			47.48	...	...
	1^-	π	g	0.6	1.03	6.84	−30.71	0.54–0.66	2.17–14.68	1.00	5.16	−28.87	0.54–0.66	1.01–12.76	0.98	6.22	−38.64	0.54–0.66	1.07–17.08
		σ	g_σ	3.4			−32.49	3.06–3.74	1.93–14.95			−24.40	3.06–3.74	1.52–11.34			−22.92	3.06–3.74	3.17–12.16
		ρ, ω	βg_V	5.2			−3.83	4.68–5.72	6.14–7.68			−2.82	4.68–5.72	4.64–5.77			−3.08	4.68–5.72	5.66–6.89
		ρ, ω	λg_V (GeV^{-1})	3.133			−3.83	2.82–3.45	6.14–7.68			−1.98	2.82–3.45	4.79–5.59			−2.77	2.82–3.45	5.72–6.83
		Kinetic energy $\langle T\rangle$ (MeV)					64.02	...	...			52.91	...	...			61.19	...	...
	2^-	π	g	0.6	1.02	6.30	−29.65	0.54–0.66	1.84–13.91	0.99	5.04	−28.61	0.54–0.66	0.95–12.58	0.95	7.05	−50.13	0.54–0.66	0.70–21.63
		σ	g_σ	3.4			−29.67	3.06–3.74	1.84–13.76			−22.48	3.06–3.74	1.66–10.74			−25.05	3.06–3.74	3.05–13.14
		ρ, ω	βg_V	5.2			−3.34	4.68–5.72	5.69–7.03			−2.43	4.68–5.72	4.59–5.56			−2.28	4.68–5.72	6.63–7.54
		ρ, ω	λg_V (GeV^{-1})	3.133			−3.30	2.82–3.45	5.70–7.03			−1.67	2.82–3.45	4.73–5.40			−3.10	2.82–3.45	6.49–7.73
		Kinetic energy $\langle T\rangle$ (MeV)					59.65	...	...			50.15	...	...			73.51	...	...
$\frac{3}{2}$	0^-	π	g	0.6	1.90	7.31	−32.13	0.54–0.66	2.31–15.32	1.89	6.91	−31.98	0.54–0.66	2.09–15.20	1.89	7.01	−32.18	0.54–0.66	2.21–15.49
		σ	g_σ	3.4			−92.22	3.20–3.74	0.15–35.37			−88.94	3.20–3.74	0.07–34.14			−89.34	3.20–3.74	0.10–34.31
		ρ, ω	βg_V	5.2			69.22	4.68–5.51	24.84–0.96			66.51	4.68–5.51	23.82–0.84			66.81	4.68–5.51	23.97–0.89
		ρ, ω	λg_V (GeV^{-1})	3.133			−54.62	2.82–3.45	0.51–23.34			−51.05	2.82–3.45	0.58–22.25			−51.41	2.82–3.45	0.67–22.65
		Kinetic energy $\langle T\rangle$ (MeV)					102.43	...	...			98.56	...	...			99.12	...	...
	1^-	π	g	0.6	1.98	7.23	−34.29	0.54–0.66	2.05–16.04	1.98	8.19	−37.21	0.54–0.66	2.49–17.62	1.98	8.19	−37.21	0.54–0.66	2.49–17.62
		σ	g_σ	3.4			−73.64	3.20–3.74	0.66–27.31			−81.33	3.20–3.74	0.79–29.84			−81.33	3.20–3.74	0.80–29.84
		ρ, ω	βg_V	5.2			58.45	4.68–5.62	21.03–0.20			64.81	4.68–5.62	23.20–0.29			64.81	4.68–5.62	23.20–0.33
		ρ, ω	λg_V (GeV^{-1})	3.133			−60.69	2.82–3.45	0.09–26.15			−68.38	2.82–3.45	0.20–29.03			−68.38	2.82–3.45	0.25–29.03
		Kinetic energy $\langle T\rangle$ (MeV)					102.95	...	...			113.92	...	...			113.92	...	...
	2^-	π	g	0.6	1.62	18.54	−82.25	0.54–0.66	5.67–38.92	1.63	21.18	−89.63	0.54–0.66	7.14–43.46	1.62	19.01	−85.33	0.54–0.66	5.86–40.52
		σ	g_σ	3.4			−201.84	3.20–3.74	0.19–70.36			−212.12	3.20–3.74	1.32–74.98			−201.46	3.20–3.74	0.57–70.73
		ρ, ω	βg_V	5.2			143.99	4.68–5.62	50.62–0.23			152.23	4.68–5.62	54.79–1.27			143.70	4.68–5.62	51.03–0.61
		ρ, ω	λg_V (GeV^{-1})	3.133			−108.11	2.82–3.45	3.62–48.58			−115.54	2.82–3.45	5.20–53.45			105.39	2.82–3.45	4.61–48.87
		Kinetic energy $\langle T\rangle$ (MeV)					229.67	...	...			243.87	...	...			229.47	...	...

TABLE VI. Dependence of binding energies on the variation of the coupling constants by about 10% for the $D^*D^*D^*$ system. The cutoff Λ, potential expectations $\langle V\rangle$, and binding energies $B^{(\prime)}$ are in units of GeV, MeV, and MeV, respectively. The binding energies B are calculated with the values of the coupling constant values given in the fifth column, and the B' are obtained within their uncertainties.

					S-wave					*S*-*D* mixing				
I	J^P	Exchanged Mesons	Coupling constant	Reference value	Λ	B	$\langle V\rangle$	Reference tange	B'	Λ	B	$\langle V\rangle$	Reference range	B'
$\frac{1}{2}$	0^-	π	g	0.6	1.07	4.48	−17.57	0.54–0.66	1.70–8.87	1.05	4.57	−20.01	0.54–0.66	1.47–9.64
		σ	g_σ	3.4			−15.00	3.06–3.74	1.94–7.97			−13.55	3.06–3.74	2.25–7.70
		ρ, ω	βg_V	5.2			−6.49	4.68–5.72	3.30–5.91			−5.56	4.68–5.72	3.56–5.79
		ρ, ω	λg_V (GeV^{-1})	3.133			−2.40	2.82–3.45	4.03–5.00			−1.60	2.82–3.45	4.27–4.92
			Kinetic energy $\langle T\rangle$ (MeV)				36.99	…	…			36.16	…	…
	1^-	π	g	0.6	1.05	5.02	−20.15	0.54–0.66	1.88–10.07	1.02	4.30	−22.03	0.54–0.66	1.08–10.05
		σ	g_σ	3.4			−23.45	3.06–3.74	1.61–11.18			−19.51	3.06–3.74	1.44–9.40
		ρ, ω	βg_V	5.2			−5.05	4.68–5.72	4.09–6.12			−3.73	4.68–5.72	3.62–5.12
		ρ, ω	λg_V (GeV^{-1})	3.133			−2.54	2.82–3.45	4.55–5.57			−1.35	2.82–3.45	4.05–4.59
			Kinetic energy $\langle T\rangle$ (MeV)				46.17	…	…			42.31	…	…
	2^-	π	g	0.6	1.03	5.94	−27.90	0.54–0.66	1.74–13.11	1.01	5.80	−30.15	0.54–0.66	1.36–13.62
		σ	g_σ	3.4			−31.72	3.06–3.74	1.29–13.98			−27.52	3.06–3.74	1.66–12.73
		ρ, ω	βg_V	5.2			−3.71	4.68–5.72	5.27–6.76			−3.10	4.68–5.72	5.23–6.47
		ρ, ω	λg_V (GeV^{-1})	3.133			−3.66	2.82–3.45	5.28–6.75			−2.33	2.82–3.45	5.37–6.30
			Kinetic energy $\langle T\rangle$ (MeV)				61.04	…	…			57.30	…	…
	3^-	π	g	0.6	1.96	6.95	−32.88	0.54–0.66	1.98–15.40	1.07	4.03	−17.33	0.54–0.66	1.32–8.39
		σ	g_σ	3.4			−73.68	3.20–3.74	0.44–27.08			−14.81	3.06–3.74	1.55–7.49
		ρ, ω	βg_V	5.2			58.27	4.68–5.62	20.73–0.02			−6.40	4.68–5.72	2.88–5.45
		ρ, ω	λg_V (GeV^{-1})	3.133			−59.30	2.88–3.45	0.71–25.39			−2.37	2.82–3.45	3.60–4.55
			Kinetic energy $\langle T\rangle$ (MeV)				100.65	…	…			36.88	…	…
$\frac{3}{2}$	1^-	π	g	0.6	1.93	5.48	−27.36	0.54–0.66	1.46–12.64	1.94	6.45	−29.86	0.54–0.66	2.07–14.40
		σ	g_σ	3.4			−67.77	3.20–3.74	0.16–26.14			−73.22	3.20–3.74	0.46–28.15
		ρ, ω	βg_V	5.2			52.33	4.68–5.51	18.73–0.72			56.68	4.68–5.62	20.49–0.19
		ρ, ω	λg_V (GeV^{-1})	3.133			−48.96	2.82–3.45	0.09–21.14			−54.19	2.82–3.45	0.35–23.87
			Kinetic energy $\langle T\rangle$ (MeV)				86.28	…	…			94.14	…	…
	2^-	π	g	0.6	1.97	7.81	−35.10	0.54–0.66	2.45–16.75	1.96	7.11	−32.58	0.54–0.66	2.25–15.67
		σ	g_σ	3.4			−77.67	3.20–3.74	0.80–28.71			−73.88	3.20–3.74	0.55–27.26
		ρ, ω	βg_V	5.2			61.67	4.68–5.62	22.21–0.30			58.44	4.68–5.62	20.91–0.13
		ρ, ω	λg_V (GeV^{-1})	3.133			−63.91	2.82–3.45	0.19–27.45			−60.23	2.82–3.45	0.14–26.29
			Kinetic energy $\langle T\rangle$ (MeV)				107.21	…	…			101.14	…	…
	3^-	π	g	0.6	1.62	19.55	−83.42	0.54–0.66	6.40–40.13	1.62	20.12	−87.08	0.54–0.66	6.62–41.99
		σ	g_σ	3.4			−209.91	3.20–3.74	0.24–72.97			−209.40	3.20–3.74	0.71–73.41
		ρ, ω	βg_V	5.2			150.08	4.68–5.62	52.77–0.26			149.69	4.68–5.62	53.25–0.72
		ρ, ω	λg_V (GeV^{-1})	3.133			−113.27	2.82–3.45	3.82–50.82			−109.99	2.82–3.45	4.98–51.12
			Kinetic energy $\langle T\rangle$ (MeV)				236.98	…	…			236.67	…	…

IV. SUMMARY

In recent years, the LHCb Collaboration achieved remarkable success in discovering new hadronic states, including many of exotic ones, which cannot fit into the conventional quark model. These observations enriched the members of the exotic hadronic family and improved our understandings of nonperturbative strong interactions. Very recently, the LHCb Collaboration observed a new state T_{cc}^+ in the $D^0D^0\pi^+$ channel [24]. The T_{cc}^+ state could well be interpreted as a DD^* molecular state and it is the first double-charm exotic state ever observed.

The observation of the T_{cc}^+ state enabled us to derive the interaction between two charmed mesons. In Ref. [30], by reproducing the binding energy of T_{cc}^+, we determined the cutoff Λ in the OBE model. This allows us to study hadronic molecular states composed of several charmed mesons. In this work, we studied the existence of triple-charm molecular states composed of D^*D^*D and $D^*D^*D^*$. Using the cutoff Λ obtained by the binding energy of the T_{cc}^+, we find that the $I(J^P) = \frac{1}{2}(0^-, 1^-, 2^-)D^*D^*D$ and $I(J^P) = \frac{1}{2}(0^-, 1^-, 2^-, 3^-)D^*D^*D$ systems have loosely bound state solutions, which could be viewed as good hadronic molecular candidates. We suggest to search for the D^*D^*D and D^*D^*D molecular states in the following decay modes:

(a) a double-charm molecular state and a charmed meson,
(b) three charmed mesons,
(c) three charmed mesons together with a number of pions and photons.

On the other hand, we find that the $I(J^P) = \frac{3}{2}(0^-, 1^-, 2^-)D^*D^*D$ and $I(J^P) = \frac{3}{2}(1^-, 2^-, 3^-)D^*D^*D^*$ systems are more difficult to form bound states.

The present framework can be extended to study the $BB^*B^* - B^*B^*B^*$ and BBB^* systems. The former has been studied in Ref. [91] and a bound state with $I(J^P) = 1/2(2^-)$ and a binding energy of 90 MeV below the lowest strong decay threshold was found. The latter has been studied in Ref. [92], where loosely bound states were found for both $I = \frac{1}{2}$ and $I = \frac{3}{2}$. The three-body systems studied in Ref. [91] are similar to those of this work, but the number of bound state solutions is far fewer than that obtained in this work. It should be noted that in the present work, we deduced the meson-meson potentials in the one-boson-exchange model, while in Ref. [91], the two-body interactions are deduced from the t matrices of Refs. [93–96]. The different meson-meson potentials are responsible for the different three-body results. In future experiments, searching for hadronic molecular candidates could help distinguish the different meson-meson interactions.

It is no doubt that the LHCb Collaboration has played an important role in searches for exotic states. The observation of the T_{cc}^+ state once again shows the capability of the LHCb detector in this area. With anticipated data accumulation [58], more exotic states can be expected in the future.

ACKNOWLEDGMENTS

This work is partly supported by the National Natural Science Foundation of China under Grants No. 11735003, No. 11975041, No. 12147152, No. 11961141004, and the Fundamental Research Funds for the Central Universities. M.-Z. L. acknowledges support from the National Natural Science Foundation of China under Grant No. 1210050997. X. L. is supported by the China National Funds for Distinguished Young Scientists under Grant No. 11825503, National Key Research and Development Program of China under Contract No. 2020YFA0406400, the 111 Project under Grant No. B20063, the National Natural Science Foundation of China under Grant No. 12047501, and the Fundamental Research Funds for the Central Universities.

[1] B. Aubert *et al.* (*BABAR* Collaboration), Observation of a Narrow Meson Decaying to $D_s^+\pi^0$ at a Mass of 2.32 GeV/c^2, Phys. Rev. Lett. **90**, 242001 (2003).
[2] D. Besson *et al.* (CLEO Collaboration), Observation of a narrow resonance of mass 2.46 GeV/c^2 decaying to $D_s^{*+}\pi^0$ and confirmation of the $D_{sJ}^*(2317)$ state, Phys. Rev. D **68**, 032002 (2003); Erratum, Phys. Rev. D **75**, 119908 (2007).
[3] S. K. Choi *et al.* (Belle Collaboration), Observation of a Narrow Charmoniumlike State in Exclusive $B^\pm \to K^\pm\pi^+\pi^- J/\psi$ Decays, Phys. Rev. Lett. **91**, 262001 (2003).
[4] T. Barnes, F. E. Close, and H. J. Lipkin, Implications of a DK molecule at 2.32 GeV, Phys. Rev. D **68**, 054006 (2003).
[5] Z. X. Xie, G. Q. Feng, and X. H. Guo, Analyzing $D_{s0}^*(2317)^+$ in the DK molecule picture in the Beth-Salpeter approach, Phys. Rev. D **81**, 036014 (2010).
[6] F. K. Guo, P. N. Shen, H. C. Chiang, R. G. Ping, and B. S. Zou, Dynamically generated 0^+ heavy mesons in a heavy chiral unitary approach, Phys. Lett. B **641**, 278 (2006).
[7] A. Faessler, T. Gutsche, V. E. Lyubovitskij, and Y. L. Ma, Strong and radiative decays of the $D_{s0}^*(2317)$ meson in the DK-molecule picture, Phys. Rev. D **76**, 014005 (2007).
[8] G. Q. Feng, X. H. Guo, and Z. H. Zhang, Studying the D^*K molecular structure of $D_{s1}^+(2460)$ in the Bethe-Salpeter approach, Eur. Phys. J. C **72**, 2033 (2012).

[9] A. Faessler, T. Gutsche, V. E. Lyubovitskij, and Y. L. Ma, D^*K molecular structure of the $D_{s1}(2460)$ meson, Phys. Rev. D **76**, 114008 (2007).

[10] Y. J. Zhang, H. C. Chiang, P. N. Shen, and B. S. Zou, Possible S-wave bound states of two pseudoscalar mesons, Phys. Rev. D **74**, 014013 (2006).

[11] E. S. Swanson, Short range structure in the $X(3872)$, Phys. Lett. B **588**, 189 (2004).

[12] C. Y. Wong, Molecular states of heavy quark mesons, Phys. Rev. C **69**, 055202 (2004).

[13] X. Liu, Z. G. Luo, Y. R. Liu, and S. L. Zhu, $X(3872)$ and other possible heavy molecular states, Eur. Phys. J. C **61**, 411 (2009).

[14] I. W. Lee, A. Faessler, T. Gutsche, and V. E. Lyubovitskij, $X(3872)$ as a molecular DD^* state in a potential model, Phys. Rev. D **80**, 094005 (2009).

[15] M. Altenbuchinger, L. S. Geng, and W. Weise, Scattering lengths of Nambu-Goldstone bosons off D mesons and dynamically generated heavy-light mesons, Phys. Rev. D **89**, 014026 (2014).

[16] H. X. Chen, W. Chen, X. Liu, and S. L. Zhu, The hidden-charm pentaquark and tetraquark states, Phys. Rep. **639**, 1 (2016).

[17] X. Liu, An overview of XYZ new particles, Chin. Sci. Bull. **59**, 3815 (2014).

[18] C. Z. Yuan, The XYZ states revisited, Int. J. Mod. Phys. A **33**, 1830018 (2018).

[19] S. L. Olsen, T. Skwarnicki, and D. Zieminska, Nonstandard heavy mesons and baryons: Experimental evidence, Rev. Mod. Phys. **90**, 015003 (2018).

[20] F. K. Guo, C. Hanhart, U. G. Meißner, Q. Wang, Q. Zhao, and B. S. Zou, Hadronic molecules, Rev. Mod. Phys. **90**, 015004 (2018).

[21] A. Hosaka, T. Iijima, K. Miyabayashi, Y. Sakai, and S. Yasui, Exotic hadrons with heavy flavors: X, Y, Z, and related states, Prog. Theor. Exp. Phys. **2016**, 062C01 (2016).

[22] N. Brambilla, S. Eidelman, C. Hanhart, A. Nefediev, C. P. Shen, C. E. Thomas, A. Vairo, and C. Z. Yuan, The XYZ states: Experimental and theoretical status and perspectives, Phys. Rep. **873**, 1 (2020).

[23] R. Aaij *et al.* (LHCb Collaboration), Observation of an exotic narrow doubly charmed tetraquark, arXiv:2109.01038.

[24] R. Aaij *et al.* (LHCb Collaboration), Study of the doubly charmed tetraquark T_{cc}^+, arXiv:2109.01056.

[25] N. Li, Z. F. Sun, X. Liu, and S. L. Zhu, Perfect DD^* molecular prediction matching the T_{cc} observation at LHCb, Chin. Phys. Lett. **38**, 092001 (2021).

[26] H. Ren, F. Wu, and R. Zhu, Hadronic molecule interpretation of T_{cc}^+ and its beauty partners, Adv. High Energy Phys. **2022**, 9103031 (2022).

[27] R. Chen, Q. Huang, X. Liu, and S. L. Zhu, Predicting another doubly charmed molecular resonance $T_{cc}'^+(3876)$, Phys. Rev. D **104**, 114042 (2021).

[28] L. R. Dai, R. Molina, and E. Oset, Prediction of new T_{cc} states of D^*D^* and $D_s^*D^*$ molecular nature, Phys. Rev. D **105**, 016029 (2022).

[29] A. Feijoo, W. H. Liang, and E. Oset, $D^0D^0\pi^+$ mass distribution in the production of the T_{cc} exotic state, Phys. Rev. D **104**, 114015 (2021).

[30] T. W. Wu, Y. W. Pan, M. Z. Liu, S. Q. Luo, L. S. Geng, and X. Liu, Discovery of the doubly charmed T_{cc}^+ state implies a triply charmed H_{ccc} hexaquark state, Phys. Rev. D **105**, L031505 (2022).

[31] R. Molina, T. Branz, and E. Oset, A new interpretation for the $D_{s2}^*(2573)$ and the prediction of novel exotic charmed mesons, Phys. Rev. D **82**, 014010 (2010).

[32] N. Li, Z. F. Sun, X. Liu, and S. L. Zhu, Coupled-channel analysis of the possible $D^{(*)}D^{(*)}$, $\bar{B}^{(*)}\bar{B}^{(*)}$ and $D^{(*)}\bar{B}^{(*)}$ molecular states, Phys. Rev. D **88**, 114008 (2013).

[33] M. Z. Liu, T. W. Wu, M. Pavon Valderrama, J. J. Xie, and L. S. Geng, Heavy-quark spin and flavor symmetry partners of the $X(3872)$ revisited: What can we learn from the one boson exchange model? Phys. Rev. D **99**, 094018 (2019).

[34] H. Xu, B. Wang, Z. W. Liu, and X. Liu, DD^* potentials in chiral perturbation theory and possible molecular states, Phys. Rev. D **99**, 014027 (2019).

[35] J. P. Ader, J. M. Richard, and P. Taxil, Do narrow heavy multiquark states exist?, Phys. Rev. D **25**, 2370 (1982).

[36] J. l. Ballot and J. M. Richard, Four quark states in additive potentials, Phys. Lett. B **123**, 449 (1983).

[37] H. J. Lipkin, A model independent approach to multiquark bound states, Phys. Lett. B **172**, 242 (1986).

[38] S. Zouzou, B. Silvestre-Brac, C. Gignoux, and J. M. Richard, Four quark bound states, Z. Phys. C **30**, 457 (1986).

[39] L. Heller and J. A. Tjon, On the existence of stable dimesons, Phys. Rev. D **35**, 969 (1987).

[40] J. Carlson, L. Heller, and J. A. Tjon, Stability of dimesons, Phys. Rev. D **37**, 744 (1988).

[41] A. V. Manohar and M. B. Wise, Exotic $QQ\bar{q}\,\bar{q}$ states in QCD, Nucl. Phys. **B399**, 17 (1993).

[42] S. Pepin, F. Stancu, M. Genovese, and J. M. Richard, Tetraquarks with color blind forces in chiral quark models, Phys. Lett. B **393**, 119 (1997).

[43] J. Vijande, A. Valcarce, and K. Tsushima, Dynamical study of bf $QQ\bar{u}\,\bar{d}$ mesons, Phys. Rev. D **74**, 054018 (2006).

[44] D. Ebert, R. N. Faustov, V. O. Galkin, and W. Lucha, Masses of tetraquarks with two heavy quarks in the relativistic quark model, Phys. Rev. D **76**, 114015 (2007).

[45] J. Vijande, A. Valcarce, and J. M. Richard, Adiabaticity and color mixing in tetraquark spectroscopy, Phys. Rev. D **87**, 034040 (2013).

[46] M. Karliner and J. L. Rosner, Discovery of Doubly Charmed Ξ_{cc} Baryon Implies a Stable $(bb\bar{u}\,\bar{d})$ Tetraquark, Phys. Rev. Lett. **119**, 202001 (2017).

[47] E. J. Eichten and C. Quigg, Heavy-Quark Symmetry Implies Stable Heavy Tetraquark Mesons $Q_iQ_j\bar{q}_k\bar{q}_l$, Phys. Rev. Lett. **119**, 202002 (2017).

[48] J. M. Richard, A. Valcarce, and J. Vijande, Few-body quark dynamics for doubly heavy baryons and tetraquarks, Phys. Rev. C **97**, 035211 (2018).

[49] W. Park, S. Noh, and S. H. Lee, Masses of the doubly heavy tetraquarks in a constituent quark model, Nucl. Phys. **A983**, 1 (2019).

[50] E. Hernández, J. Vijande, A. Valcarce, and J. M. Richard, Spectroscopy, lifetime and decay modes of the T_{bb}^- tetraquark, Phys. Lett. B **800**, 135073 (2020).

[51] X. Z. Ling, M. Z. Liu, L. S. Geng, E. Wang, and J. J. Xie, Can we understand the decay width of the T_{cc}^+ state? Phys. Lett. B **826**, 136897 (2022).

[52] R. Aaij *et al.* (LHCb Collaboration), Observation of $J/\psi p$ Resonances Consistent with Pentaquark States in $\Lambda_b^0 \to J/\psi K^- p$ Decays, Phys. Rev. Lett. **115**, 072001 (2015).

[53] R. Aaij *et al.* (LHCb Collaboration), Observation of a Narrow Pentaquark State, $P_c(4312)^+$, and of Two-Peak Structure of the $P_c(4450)^+$, Phys. Rev. Lett. **122**, 222001 (2019).

[54] R. Aaij *et al.* (LHCb Collaboration), Evidence of a $J/\psi\Lambda$ structure and observation of excited Ξ^- states in the $\Xi_b^- \to J/\psi\Lambda K^-$ decay, Sci. Bull. **66**, 1278 (2021).

[55] R. Aaij *et al.* (LHCb Collaboration), A Model-Independent Study of Resonant Structure in $B^+ \to D^+D^-K^+$ Decays, Phys. Rev. Lett. **125**, 242001 (2020).

[56] R. Aaij *et al.* (LHCb Collaboration), Amplitude analysis of the $B^+ \to D^+D^-K^+$ decay, Phys. Rev. D **102**, 112003 (2020).

[57] R. Aaij *et al.* (LHCb Collaboration), Observation of structure in the J/ψ -pair mass spectrum, Sci. Bull. **65**, 1983 (2020).

[58] R. Aaij *et al.* (LHCb Collaboration), Physics case for an LHCb Upgrade II—Opportunities in flavour physics, and beyond, in the HL-LHC era, arXiv:1808.08865.

[59] D. O. Riska and G. E. Brown, Nucleon resonance transition couplings to vector mesons, Nucl. Phys. **A679**, 577 (2001).

[60] M. Gell-Mann and M. Levy, The axial vector current in beta decay, Nuovo Cimento **16**, 705 (1960).

[61] C. Isola, M. Ladisa, G. Nardulli, and P. Santorelli, Charming penguins in $B \to K^*\pi, K(\rho, \omega, \phi)$ decays, Phys. Rev. D **68**, 114001 (2003).

[62] P. A. Zyla *et al.* (Particle Data Group), Review of particle physics, Prog. Theor. Exp. Phys. **2020**, 083C01 (2020).

[63] E. Hiyama, Y. Kino, and M. Kamimura, Gaussian expansion method for few-body systems, Prog. Part. Nucl. Phys. **51**, 223 (2003).

[64] E. Hiyama, Gaussian expansion method for few-body systems and its applications to atomic and nuclear physics, Prog. Theor. Exp. Phys. **2012**, 01A204 (2012).

[65] T. Yoshida, E. Hiyama, A. Hosaka, M. Oka, and K. Sadato, Spectrum of heavy baryons in the quark model, Phys. Rev. D **92**, 114029 (2015).

[66] G. Yang, J. Ping, P. G. Ortega, and J. Segovia, Triply heavy baryons in the constituent quark model, Chin. Phys. C **44**, 023102 (2020).

[67] G. Yang, J. Ping, and J. Segovia, The S- and P-wave low-lying baryons in the chiral quark model, Few Body Syst. **59**, 113 (2018).

[68] G. Yang, J. Ping, and J. Segovia, $sQ\bar{q}\,\bar{q}$ $(q = u, d; Q = c, b)$ tetraquarks in the chiral quark model, Phys. Rev. D **103**, 074011 (2021).

[69] G. Yang, J. Ping, and J. Segovia, $QQ\bar{s}\,\bar{s}$ tetraquarks in the chiral quark model, Phys. Rev. D **102**, 054023 (2020).

[70] G. J. Wang, L. Meng, and S. L. Zhu, Spectrum of the fully-heavy tetraquark state $QQ\bar{Q}'\bar{Q}'$, Phys. Rev. D **100**, 096013 (2019).

[71] Q. F. Lü, D. Y. Chen, Y. B. Dong, and E. Santopinto, Triply-heavy tetraquarks in an extended relativized quark model, Phys. Rev. D **104**, 054026 (2021).

[72] Q. F. Lü, D. Y. Chen, and Y. B. Dong, Masses of fully heavy tetraquarks $QQ\bar{Q}\,\bar{Q}$ in an extended relativized quark model, Eur. Phys. J. C **80**, 871 (2020).

[73] T. W. Wu, M. Z. Liu, L. S. Geng, E. Hiyama, and M. P. Valderrama, DK, DDK, and $DDDK$ molecules—Understanding the nature of the $D_{s0}^*(2317)$, Phys. Rev. D **100**, 034029 (2019).

[74] T. W. Wu, M. Z. Liu, L. S. Geng, E. Hiyama, M. P. Valderrama, and W. L. Wang, Quadruply charmed dibaryons as heavy quark symmetry partners of the DDK bound state, Eur. Phys. J. C **80**, 901 (2020).

[75] T. W. Wu, M. Z. Liu, and L. S. Geng, Excited K meson, $K_c(4180)$, with hidden charm as a $D\bar{D}K$ bound state, Phys. Rev. D **103**, L031501 (2021).

[76] T. W. Wu, Y. W. Pan, M. Z. Liu, J. X. Lu, L. S. Geng, and X. H. Liu, Hidden charm hadronic molecule with strangeness $P_{cs}^*(4739)$ as a $\Sigma_c\bar{D}\,\bar{K}$ bound state, Phys. Rev. D **104**, 094032 (2021).

[77] T. W. Wu and L. S. Geng, Study on triple-hadron bound states with Gaussian expansion method, Few Body Syst. **62**, 89 (2021).

[78] T. W. Wu, M. Z. Liu, and L. S. Geng, One way to verify the molecular picture of exotic hadrons: From DK to $DDK/D\bar{D}^{(*)}K$, Few Body Syst. **62**, 38 (2021).

[79] D. M. Brink and F. Stancu, Tetraquarks with heavy flavors, Phys. Rev. D **57**, 6778 (1998).

[80] G. E. Brown and W. Weise, Pion scattering and isobars in nuclei, Phys. Rep. **22**, 279 (1975).

[81] A. M. Green and P. Haapakoski, The effect of the $\Delta(1236)$ in the two-nucleon problem and in neutron matter, Nucl. Phys. **A221**, 429 (1974).

[82] P. Haapakoski, A nucleon-nucleon potential that includes the effect of the $N^*(1236)$, Phys. Lett. **48B**, 307 (1974).

[83] A. M. Green and J. A. Niskanen, The saturating effect of the $\Delta(1236)$ in nuclear matter, Nucl. Phys. **A249**, 493 (1975).

[84] W. Meguro, Y. R. Liu, and M. Oka, Possible $\Lambda_c\Lambda_c$ molecular bound state, Phys. Lett. B **704**, 547 (2011).

[85] N. A. Tornqvist, Possible Large Deuteronlike Meson-Meson States Bound by Pions, Phys. Rev. Lett. **67**, 556 (1991).

[86] R. Chen, X. Liu, X. Q. Li, and S. L. Zhu, Identifying Exotic Hidden-Charm Pentaquarks, Phys. Rev. Lett. **115**, 132002 (2015).

[87] R. Chen, Z. F. Sun, X. Liu, and S. L. Zhu, Strong LHCb evidence supporting the existence of the hidden-charm molecular pentaquarks, Phys. Rev. D **100**, 011502 (2019).

[88] R. Chen, F. L. Wang, A. Hosaka, and X. Liu, Exotic triple-charm deuteronlike hexaquarks, Phys. Rev. D **97**, 114011 (2018).

[89] R. Chen, A. Hosaka, and X. Liu, Prediction of triple-charm molecular pentaquarks, Phys. Rev. D **96**, 114030 (2017).

[90] S. Yasui and K. Sudoh, Exotic nuclei with open heavy flavor mesons, Phys. Rev. D **80**, 034008 (2009).

[91] H. Garcilazo and A. Valcarce, T_{bbb}: A three B–meson bound state, Phys. Lett. B **784**, 169 (2018).

[92] L. Ma, Q. Wang, and U. G. Meißner, Trimeson bound state BBB^* via a delocalized π bond, Phys. Rev. D **100**, 014028 (2019).

[93] J. Vijande, A. Valcarce, and N. Barnea, Exotic meson-meson molecules and compact four-quark states, Phys. Rev. D **79**, 074010 (2009).

[94] J. Vijande and A. Valcarce, Probabilities in nonorthogonal basis: Four-quark systems, Phys. Rev. C **80**, 035204 (2009).

[95] T. F. Carames, A. Valcarce, and J. Vijande, Too many $X's$, $Y's$ and $Z's$?, Phys. Lett. B **709**, 358 (2012).

[96] H. Garcilazo, A. Valcarce, and T. F. Caramés, Three-body systems with open flavor heavy mesons, Phys. Rev. D **96**, 074009 (2017).